Topical Report 1

High-Pressure Turbulent Flame Speeds and Chemical Kinetics of Syngas Blends with and without Impurities

For the Period:
October 1, 2013 – September 30, 2014

Principal Authors:
Eric Petersen, Olivier Mathieu, Anibal Morones, Sankar Ravi, Charles Keesee, Joshua Hargis, and Jose Vivanco

Principal Investigator:
Eric L. Petersen
Department of Mechanical Engineering
Texas A&M University
3123 TAMU
College Station, TX 77843
407-823-6123

Issue Date: November 2014

DOE Award No. DE-FE0011778
TEES Project 32525-C2920

Texas A&M Engineering Experiment Station
400 Harvey Mitchell Parkway, Suite 300
College Station, TX 77845-4375

ABSTRACT

This Topical Report documents the first year of the project, from October 1, 2013 through September 30, 2014. Efforts for this project included experiments to characterize the atmospheric-pressure turbulent flame speed vessel over a range of operating conditions (fan speeds and turbulent length scales). To this end, a new LDV system was acquired and set up for the detailed characterization of the turbulence field. Much progress was made in the area of impurity kinetics, which included a numerical study of the effect of impurities such as NO_2, NO, H2S, and NH_3 on ignition delay times and laminar flame speeds of syngas blends at engine conditions. Experiments included a series of laminar flame speed measurements for syngas (CO/H_2) blends with various levels of CH_4 and C_2H_6 addition, and the results were compared to the chemical kinetics model of NUI Galway. Also, a final NOx kinetics mechanism including ammonia was assembled, and a journal paper was written and is now in press. Overall, three journal papers and six conference papers related to this project were published this year. Finally, much progress was made on the design of the new high-pressure turbulent flame speed facility. An overall design that includes a venting system was decided upon, and the detailed design is in progress.

TABLE OF CONTENTS

EXECUTIVE SUMMARY

This Topical Report documents the first year of the project, from October 1, 2013 through September 30, 2014. This effort is concerned with the chemical kinetics of fuel blends with high-hydrogen content in the presence of impurities. Emphasis is on the design and construction of a high-pressure turbulent flame speed facility and the use of ignition delay times and flame speeds to elucidate the diluent and impurity effects on the fuel chemistry at gas turbine engine conditions and to also validate the chemical kinetics models. The project is divided into five primary tasks: 1) Project Management and Program Planning; 2) Turbulent Flame Speed Measurements at Atmospheric Pressure; 3) Experiments and Kinetics of Syngas Blends with Impurities; 4) Design and Construction of a High-Pressure Turbulent Flame Speed Facility; and 5) High-Pressure Turbulent Flame Speed Measurements.

Besides mostly H_2 and CO, syngas also contains reasonable amounts of light hydrocarbons, CO_2, H_2O, N_2, and Ar. Impurities such as NH_3, HCN, COS, H_2S, and NOx (NO, NO_2, N_2O) are also commonly found in syngas. The presence of these impurities, even in very low concentrations, can induce some strong changes in combustion properties. Although they introduce potential design and operational issues for gas turbines, these changes in combustion properties due to the presence of impurities are still not well characterized. The aim of this work was therefore to investigate numerically the effect of the presence of impurities in realistic syngas compositions on some fundamental combustion properties of premixed systems such as laminar flame speed and ignition delay time, at realistic engine operating conditions. To perform this study, a state-of-the-art C0-C3 detailed kinetics mechanism was used. This mechanism was combined with recent, optimized sub-mechanisms for impurities which can impact the combustion properties of the syngas such as nitrogenous species (i.e., N_2O, NO_2, NH_3, and HCN) and sulfur-based species such as H_2S, SO_2 and COS. Several temperatures, pressures, and equivalence ratios were investigated. The results of this study showed that the addition of some impurities modifies notably the reactivity of the mixture. The ignition delay time is decreased by the addition of NO_2 and H_2S at the temperatures and pressures for which the HO_2 radical dominates the H_2 combustion. However, while NO_2 has no effect when OH is dominating, H_2S increases the ignition delay time in such conditions for pressures above 1 atm. The amplitude of these effects is however dependent on the impurity concentration. Laminar flame speeds are not sensitive to NO_2 addition but NH_3 and HCN are, inducing a small reduction of the laminar flame speed at fuel rich conditions. H_2S exhibits some inhibiting effects on the laminar flame speed but only for high concentrations. The inhibiting effects of NH_3, HCN, and H_2S are due to the OH radical consumption by these impurities, leading to radicals that are less reactive.

New Laminar Flame Speed measurements have been taken for a wide range of syngas mixtures containing hydrocarbon impurities. These experiments encompassed a wide range of syngas mixtures beginning with two baseline mixtures. The first of these baseline mixtures was a bio-syngas with a 50/50 H_2/CO split, and the second baseline mixture was a coal syngas with a 40/60 H_2/CO split. Experiments were conducted over a range of equivalence ratios from ϕ = 0.5 to 3 at initial conditions of 1 atm and 300 K. Upon completion of the baseline experiments, two different hydrocarbons were added to the fuel mixtures at levels ranging from 0.8 to 15% by volume, keeping the H_2/CO ratio locked for the bio-syngas and coal syngas mixtures. The addition of these light hydrocarbons, namely CH_4 and C_2H_6, had been shown in recent calculations by the authors' groups to have significant impacts on the laminar flame speed, and

the present experiments validated the suspected trends. For example, a 7% addition of methane to the coal-syngas blend decreased the peak flame speed by about 25% and shifted it from ϕ = 2.2 to a leaner value near ϕ = 1.5. Also, the addition of ethane at 1.7% reduced the mixture flame speed more than a similar addition of methane (1.6%). In general, the authors' chemical kinetic model over predicted the laminar flame speed by about 10-20% for the mixtures containing the hydrocarbons. The decrease in laminar flame speed with the addition of the hydrocarbons can be explained by the increased importance of the inhibiting reaction $CH_3 + H (+M) \leftrightarrow CH_4 (+M)$, which also explains the enhanced effect of C_2H_6 compared CH_4, where the former produces more CH_3 radicals, particularly at fuel rich conditions.

Much progress has been made on the design of the new turbulent flame speed rig for elevated pressures, and a detailed summary of the current design is provided in this report. A conceptual design has been derived, and the detailed design is underway.

APPROACH

The basic approach is best summarized by the five main tasks, as follows.

Task 1 – Project Management and Program Planning
Project management includes the submission of regular and required reports to DOE, in addition to routine management of the TAMU project by the PI. This task also includes the specific interaction with the industry consultants. Feedback from Rolls-Royce, Alstom, and GE will be obtained at the beginning of the program through face-to-face meetings, followed by periodic contact throughout the project.

Task 2 – Turbulent Flame Speed Measurements at Atmospheric Pressure
Using the original turbulent flame speed vessel at that was developed under a previous UTSR grant, we will perform turbulent flame speed measurements for a range of syngas blends at atmospheric pressure. Turbulence is generated with fans, and the experiments for the current project will include a range of both turbulent intensity and length scale. Correlations will be developed that relate the turbulent speed to the equivalent laminar flame speed for the same mixture and initial pressure. Any parallel DOE-UTSR projects that are also focusing on turbulent flame speeds, particularly those using different measurement approaches, will be monitored so that complementary and overlapping results can be obtained as applicable.

Task 3 – Experiments and Kinetics of Syngas Blends with Impurities
These experiments will involve shock-tubes and laminar flame speed vessels to obtain data 1) assessing the impact of likely impurities, and 2) validating the various kinetics sub-mechanisms for each impurity at realistic ranges of mixture composition, stoichiometry, and pressure. Emphasis will be placed on: 1) ignition experiments (both dilute and high concentration) containing initial levels of impurities, to obtain ignition delay times for a global assessment of the chemistry; 2) dilute experiments wherein key intermediate species profiles are measured using absorption spectroscopy; and 3) laminar flame speed experiments at elevated pressure and temperature. The resulting database will be compared to the main syngas/NOx mechanism combined with the impurity sub-mechanisms, and areas for improvement will be identified.

Task 4 – Design and Construction of a High-Pressure Turbulent Flame Speed Facility
This task involves the design, construction, and characterization of a new turbulent flame speed vessel capable of initial pressures as high as 20 atm. We intend to use a technique with a secondary chamber to exhaust the high-pressure gases during the combustion process, hence reducing or completely eliminating the high overpressure. The basic fan design and construction details will take advantage of our existing tools and experiences in this area.

Task 5 – High-Pressure Turbulent Flame Speed Measurements
This task will involve primarily the turbulent flame speed measurements using the new facility developed and demonstrated in Task 4. We anticipate that these tests will commence in Year 3, but they could be performed sooner if Task 4 is completed ahead of schedule, which is likely. A large part of the effort will be focused on correlating the resulting high-pressure data. As needed, for every set of conditions in the turbulent flame speed experiment, an equivalent laminar flame speed experiment will have to be performed to provide the reference condition for comparison.

RESULTS AND DISCUSSION

Progress during this first year of the project is presented within the context of the six primary tasks.

TASK 1 – PROJECT MANAGEMENT AND PROGRAM PLANNING

On April 3, 2014, the PI gave an update presentation to DOE NETL representatives over the telephone and computer. From Aug. 3 through Aug. 8, 2014, the PI attended the 35th International Symposium on Combustion, in San Francisco, CA. Several students also attended the symposium and presented three posters related to the current work, also listed below.

Journal Publications this Year

During this second year of the project effort, we have published 3 journal articles related to the project (2 in print, with 1 more submitted and now in press). These papers are summarized below.

1. O. Mathieu, E. L. Petersen, A. Heufer, N. Donohoe, W. Metcalfe, H. J. Curran, F. Güthe, and G. Bourque, "Numerical Study on the Effect of Real Syngas Compositions on Ignition Delay Times and Laminar Flame Speeds at Gas Turbine Conditions," *Journal of Engineering for Gas Turbines and Power*, Vol. 136, 2014, pp. 011502-(9).

2. O. Mathieu, F. Deguillaume, and E. L. Petersen, "Effects of H_2S Addition on Hydrogen Ignition behind Reflected Shock Waves: Experiments and Modeling," *Combustion and Flame*, Vol. 161, 2014, pp. 23-36.

3. O. Mathieu and E. L. Petersen, "Experimental and Modeling Study on the High-Temperature Oxidation of Ammonia and Related NOx Chemistry," *Combustion and Flame*, in press.

Conference Papers and Presentations this Year

Six conference papers were presented that were related to the work of this project, summarized below. The paper listed under the International Symposium on Combustion will also appear later in the journal *Proceedings of the Combustion Institute*.

1. O. Mathieu, J. Hargis, A. Camou, C. Mulvihill, and E. L. Petersen, "Ignition Delay Time Measurements Behind Reflected Shock Waves for a Representative Coal-Derived Syngas With and Without NH_3 and H_2S Impurities," Spring Technical Meeting of the Central States Section of the Combustion Institute, Tulsa, Oklahoma, March 16-18, 2014.

2. E. Vivanco, D. Pastrich, J. Anderson, and E. L. Petersen, "A New Shock-Tube Facility for the Study of High-Temperature Chemical Kinetics," Spring Technical Meeting of the Central States Section of the Combustion Institute, Tulsa, Oklahoma, March 16-18, 2014.

3. C. Mulvihill, C. Aul, S. Thion, and E. L. Petersen, "Using UV Absorption Spectroscopy to Measure the Time History of the Hydroxyl Radical in a Shock Tube," Spring

Technical Meeting of the Central States Section of the Combustion Institute, Tulsa, Oklahoma, March 16-18, 2014.

4. O. Mathieu, E. L. Petersen, H. J. Curran, F. Güthe, and G. Bourque, "The Effect of Impurities on Ignition Delay Times and Laminar Flame Speeds of Syngas Mixtures at Gas Turbine Conditions," ASME Paper GT2014-25411, ASME Turbo Expo 2014, June 16-20, 2014, Düsseldorf, Germany.

5. Morones, S. Ravi, D. Plichta, E. L. Petersen, H. J. Curran, G. Bourque, F. Güthe, and T. Wind, "Laminar and Turbulent Flame Speed Measurements and Modeling for Natural Gas/Hydrogen Blends at Elevated Pressures," ASME Paper GT2014-26742, ASME Turbo Expo 2014, June 16-20, 2014, Düsseldorf, Germany.

6. O. Mathieu, J. W. Hargis, A. Camou, C. Mulvihill, and E. L. Petersen, "Ignition Delay Time Measurements Behind Reflected Shock Waves for a Representative Coal-Derived Syngas With and Without NH_3 and H_2S Impurities," 35th International Symposium on Combustion, San Francisco, CA, Aug. 3-8, 2014.

Poster Presentations this Year

1. J. E. Vivanco, D. Pastrich, J. Anderson, K. Letourneau, and E. L. Petersen, "A New Shock-Tube Facility for the Study of High-Temperature Chemical Kinetics," Work in Progress Poster presentation, 35th International Symposium on Combustion, San Francisco, CA, Aug. 3-8, 2014.

2. C. L. Keesee and E. L. Petersen, "Laminar Flame Speed Measurements of Synthetic Gas Blends with and without Impurities," Work in Progress Poster presentation, 35th International Symposium on Combustion, San Francisco, CA, Aug. 3-8, 2014.

3. S. Ravi, A. Morones, E. L. Petersen, and F. Güthe, "Turbulent Displacement Speeds of a Natural Gas Surrogate with Hydrogen Addition," Work in Progress Poster presentation, 35th International Symposium on Combustion, San Francisco, CA, Aug. 3-8, 2014.

TASK 2 – TURBULENT FLAME SPEED MEASUREMENTS AT ATMOSPHERIC PRESSURE

The laser Doppler velocimeter system arrived in August, and it is being set up for use on the existing turbulent flame speed rig to characterize the flow field over a range of fan settings. Figure 1 shows the LDV lasers in action. Most of the time over August and September were been spent in optimizing the measurements within the constraints of the vessel geometry and flow conditions, including the proper alignment of the optics to avoid and reduce reflections and scattering and the optimal setting of the suspended tracer particles.

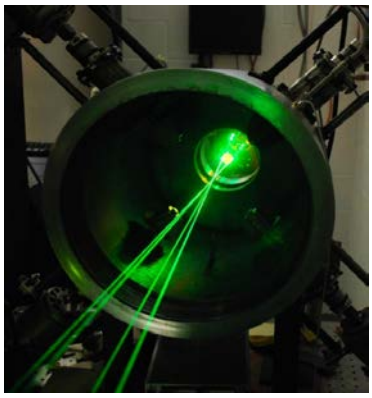

Fig. 1 2D LDV beams in place on the turbulent flame speed rig. The endcap was removed for clarity in this picture.

Measurements along the axial centerline, depicted in Fig. 2, have been performed for the fan settings defined in Ravi et al. (2013). The LDV results thus far are summarized in Fig. 3. Although is a slight deviation in the rms velocity, the average velocity remains near zero, as expected and as measured in the PIV experiments of Ravi et al. (2013). Further results will be presented early in the second year of the project.

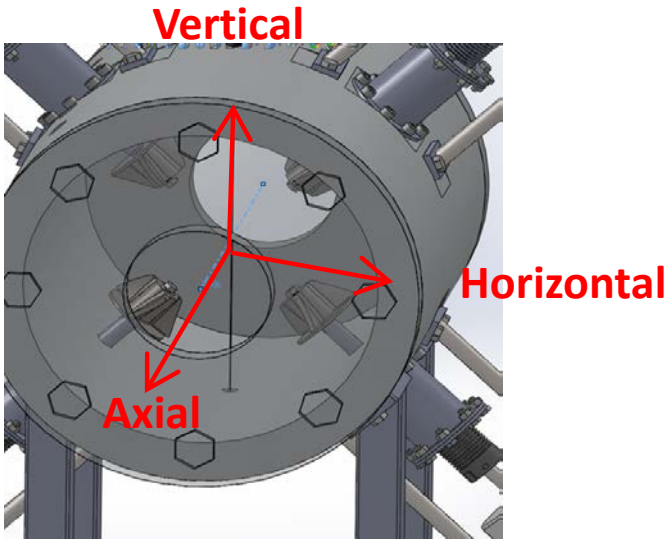

Fig. 2 Turbulent flame speed vessel coordinate system. The origin is located at the geometrical center. Velocities V1 (horizontal) and V2 (vertical) were measured with LDV (and PIV) techniques.

.

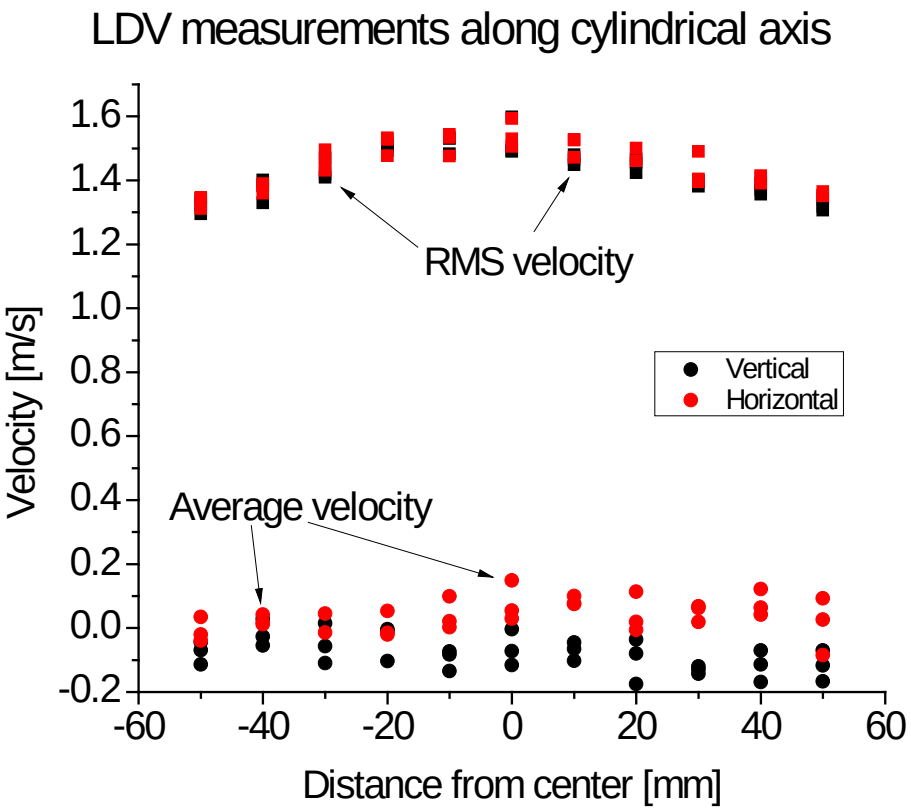

Fig. 3 RMS values of velocity show a slight decline as we move away from the center. However, the average value, stays close to zero.

TASK 3 – EXPERIMENTS AND KINETICS OF SYNGAS BLENDS WITH IMPURITIES

This task is focused on the measurement of laminar flame speed and ignition delay time for syngas mixtures with various impurities; chemical kinetics modeling is ultimately what the data are used to improve and to which they are compared. Two main projects were completed, the first dealing with the use of our improved NOx and impurities kinetics mechanisms to perform calculations at gas turbine conditions to assess the effect of the impurities. The second was concerned with the measurement of laminar flame speeds for syngas blends with hydrocarbon addition.

Effect of Impurities at Gas Turbine Conditions

Synthetic gas or syngas can be produced from nearly any type of carbonaceous feedstock. This wide array of possible sources in particular makes syngas an attractive fuel for dependable, clean, and efficient energy production using Integrated Gasification Combined Cycle (IGCC) plants or gas turbines. The syngas composition depends on the type of feedstock and on the process used to gasify it. The composition can include 6.8%–50.4% H_2, 8.1%–60.5% CO, 1.3%–29.6% CO_2, 0%–20.4% H_2O, 0%–9.3% CH_4 [Kreji et al., 2013], and many impurities. Despite this complex composition, most of the studies on syngas have been historically focusing on H_2/CO only. Few studies have also dealt with steam [Das et al., 2011], CO_2 [Burke et al., 2007; Natarajan et al., 2005; Wang et al., 2013], N_2 [Prathap et al., 2008], or realistic mixture composition (although highly diluted in Ar for the shock-tube data) [Herzler et al., 2012; Mathieu et al., 2013a].

Recently, the effects of hydrocarbon addition (CH_4, C_2H_6, C_2H_4, and C_2H_2) were studied numerically at realistic gas turbine conditions for a series of syngas compositions (from the baseline CO/H_2 to real syngas mixture compositions) derived from biomass and coal feedstocks by the present authors [Mathieu et al., 2013b]. The results of this study exhibited the great importance of hydrocarbons, even in small concentration, on fundamental combustion properties such as ignition delay time (τ_{ign}) and laminar flame speed (S_L). Indeed, while the CO/H_2 ratio was found to be of little importance on the ignition delay time, the addition of hydrocarbons increased τ_{ign} notably under the conditions investigated. This increase was a function of the nature and concentration of the hydrocarbon and the pressure and temperature range. At 1 atm, the ignition delay time was increased over the entire range of temperatures studied, whereas τ_{ign} was increased only on the high-temperature side at 10 and 35 atm. This effect of the ignition delay time was mostly due to methane and ethylene. For the flame speed, however, ethane was found to be of larger importance, with a noticeable decrease in S_L. It was demonstrated in this previous study that the effects of the hydrocarbon addition are mostly due to reactions between the hydrocarbons and/or their radicals with the radical H, hence competing with the most important promoting reaction $H + O_2 \rightleftarrows OH + O$ at the conditions of interest to gas turbine combustors.

The comparison between the baseline coal- and bio-derived syngases with averaged syngases (containing hydrocarbons, CO_2, H_2O, N_2) showed a large difference in the ignition delay time and in the flame speed. The impacts on the flame speed were due to both chemical and thermal (i.e. flame temperature) effects, whereas the effects on the ignition delay time were linked to the chemistry only. The main outcome of that recent study was that the baseline CO/H_2 mixtures

generally studied are not in many cases good candidates to study syngas combustion under gas turbine conditions because they represent an over-simplified blend.

As mentioned earlier, in addition to these fuels and diluents, traces of impurities can also be found in syngas. These impurities are typically NH_3, HCN, COS, H_2S, SO_2, and NOx (NO, NO_2, N_2O), although some traces of HCl and metals have also been reported [Newby et al., 2001; Trembly et al., 2007]. While the concentration of these impurities is typically very low (up to 1.3% and 0.3% vol. for H_2S and HCN, respectively [Cayana et al., 2008], 1.64% vol. for NH_3 [Cuoci et al., 2007], 0.055 % vol. for SO_2 and 0.123 % vol. for NOx [Xu et al., 2011]), they can have a great impact on fuel combustion properties [Glarborg, 2007]. It is also worth mentioning that the combustion properties of syngas are, in most cases, driven by hydrogen combustion chemistry [Krejci et al., 2013; Kéromnès et al., 2013; Mathieu et al., 2013b]. Recent studies with H_2 mixtures seeded with small amounts of NO_2 [Mathieu et al., 2013c] and H_2S [Mathieu et al., 2013d] exhibited a great influence of these impurities on the ignition delay time (generally promoting for NO_2 and generally inhibiting for H_2S). However, except for NH_3 [Mathieu et al., 2013a], there is no study on the influence of these impurities on realistic syngas combustion. There is also no study on the potential interactions between these impurities during syngas combustion.

Since kinetics models for these impurities have been recently optimized (Mathieu et al. for NO_2 (2013c), N_2O (2012), H_2S (2013d), NH_3/H_2-NOx, Dagaut et al. (2008) for HCN, and Glarborg and Marshall (2013) for COS), it is now possible to investigate numerically, with a reasonable degree of accuracy, the effects of these impurities on syngas combustion properties. The aim of the present study was therefore to perform such a numerical investigation for fundamental combustion properties of premixed systems, i,e, laminar flame speed and ignition delay time. Realistic engine operating conditions were selected, and various syngas compositions were studied.

The syngas compositions defined in Mathieu et al. (2013b) were used to define neat baselines for bio- and coal-derived syngases herein. These baseline mixtures were then computationally seeded with various impurities specific to each type of syngas to exhibit their effects on combustion properties of interest herein. The mixtures investigated and the modeling procedure details are covered first in this section of the report. Results are then presented and discussed, with emphasis on the significant chemical kinetics reactions.

Modeling Procedure. The detailed chemical kinetics model used herein is based on the C0–C3 mechanism developed at the National University of Ireland, Galway (NUIG) [Metcalfe et al., 2013]. A high-temperature version of this model, where low-temperature species (peroxy radicals, alkyl hydroperoxides, ketohydroperoxides, etc.) and reactions were removed, was used for flame speed calculations. To this base mechanism were added the sub-mechanisms for H_2/H_2S [Mathieu et al., 2013d] and NH_3-H_2/NOx. The HCN mechanism was added to the NH_3 part and has been unchanged from the work of Dagaut et al. (2008). The COS sub-mechanism is from a recent paper from Glarborg and Marshall (2013), while the NOx-HC interactions were taken from the work of Sivaramakrishnan et al. (2007). The complete mechanism comprises 1,331 reactions and 198 species, while the high-temperature mechanism consists of 188 species and 1,243 reactions. The modeling of the various syngas mixture was done with air as the

oxidant. The Chemkin package 10112 was used to perform the numerical calculations. Ignition delay time calculations were performed using the Closed Homogeneous Batch Reactor model with the Constant Volume assumption, while the Premixed Laminar Flame Speed Calculation model was used to compute the laminar flame speeds.

Mixtures Investigated. The two first mixtures studied were the baseline (CO/H_2) coal- and bio-derived syngas mixtures in air (60/40 and 50/50 (mole ratio), respectively). These neat mixtures were then seeded with single impurities (COS, NH_3, and H_2S for the coal syngas and NO_2, NH_3, HCN, and SO_2 for the bio-syngas) at their maximum reported concentration in the literature to estimate the effect of impurities on ignition delay time and laminar flame speed on these baseline mixtures. Note that due to their possible large concentration and presumably great effects on combustion properties, NO_2 and H_2S have also been studied at averaged concentrations that have been determined from several syngas mixture compositions [Munasinghe and Khanal, 2010; Xu et al., 2009; Sharma et al., 2013; Newby et al., 2001]. For each type of syngas, a mixture containing all the aforementioned impurities at their maximum reported concentration was also investigated, to exhibit possible synergistic or antagonistic effects between impurities.

In addition to these baseline syngases, averaged, realistic, neat mixtures, containing H_2/CO, H_2O, N_2, CO_2, and small hydrocarbons were also defined. More details on these realistic mixtures and on the effects of hydrocarbons on ignition delay time and laminar flame speed are available in Mathieu et al. (2013b). Effects of NO_2 and H_2S at averaged and maximum reported concentrations for, respectively, these realistic bio- and coal-derived syngases were investigated. Finally, the realistic syngases were also studied with the maximum reported concentration of all impurities specific to each type of syngas. The compositions of the mixtures investigated in this study are provided in Table 1 for the bio-derived syngas and in Table 2 for the coal-derived syngas.

Table 1 Bio-syngas mixtures investigated (mole fraction).

Mixture	H_2	CO	CH_4	C_2H_6	C_2H_4	C_2H_2	H_2O	N_2	CO_2	NO_2	NH_3	HCN	SO_2
bBiosyn	50.0	50.0	—	—	—	—	—	—	—	—	—	—	—
bBiosyn-HC	39.1	39.1	15.0	0.8	5.3	0.7	—	—	—	—	—	—	—
bBiosyn-NO_2Av	49.98	49.98	—	—	—	—	—	—	—	0.04	—	—	—
bBiosyn-NO_2Hi	49.94	49.94	—	—	—	—	—	—	—	0.12	—	—	—
bBiosyn-NH_3	49.86	49.86	—	—	—	—	—	—	—	—	0.28	—	—
bBiosyn-HCN	49.86	49.86	—	—	—	—	—	—	—	—	—	0.28	—
bBiosyn-SO_2	49.9725	49.9725	—	—	—	—	—	—	—	—	—	—	0.055
bBiosyn-impur	49.6325	49.6325	—	—	—	—	—	—	—	0.12	0.28	0.28	0.055
Biosyn	21.75	21.75	8.5	—	—	—	20.0	13.0	15.0	—	—	—	—
Biosyn-NO_2Av	21.7413	21.7413	8.4966	—	—	—	19.992	12.995	14.994	0.04	—	—	—
Biosyn-NO_2Hi	21.7239	21.7239	8.4898	—	—	—	19.976	12.984	14.982	0.12	—	—	—
Biosyn-impur	21.5901	21.5901	8.4375	—	—	—	19.853	12.905	14.8898	0.12	0.28	0.28	0.055

Flame speed computations were performed at 1 and 15 atm; between ϕ = 0.5 and 3.0; and for unburned gas temperatures (T_u) of 300 and 500 K. Ignition delay time computations were performed between 900 and 1400 K; at 1, 10, and 35 atm; and for an equivalence ratio of ϕ = 0.5. Stoichiometric mixtures were also investigated for the neat mixtures as well as for the mixtures with all the impurities. The ignition delay time was defined by the step rise in the OH* signal, which occurs at ignition, as visible in Fig. 4. As can be seen in this figure, a similar result would

have been obtained using the pressure signal, even though a slow and very moderate pressure increase can be observed before the ignition.

Table 2 Coal-syngas mixtures investigated (mole fraction).

Mixture	H_2	CO	CH_4	C_2H_6	C_2H_4	C_2H_2	H_2O	N_2	CO_2	COS	H_2S	NH_3
bCoalsyn	40.00	60.00	—	—	—	—	—	—	—	—	—	—
bCoalsyn-HC	36.268	54.402	7.4	1.7	0.1	0.13	—	—	—	—	—	—
bCoalsyn-COS	39.996	59.994	—	—	—	—	—	—	—	0.01	—	—
bCoalsyn-H_2SAv	39.996	59.994	—	—	—	—	—	—	—	—	0.01	—
bCoalsyn-H_2SHi	39.6	59.4	—	—	—	—	—	—	—	—	1	—
bCoalsyn-NH_3	39.84	59.76	—	—	—	—	—	—	—	—	—	0.4
bCoalsyn-impur	39.436	59.154	—	—	—	—	—	—	—	0.01	1	0.4
Coalsyn	23.48	35.22	1.6	—	—	—	21.8	8.5	9.4	—	—	—
Coalsyn-H_2SAv	23.4777	35.2165	1.5998	—	—	—	21.7978	8.4991	9.3991	—	0.01	—
Coalsyn-H_2SHi	23.2452	34.8678	1.584	—	—	—	21.582	8.415	9.306	—	1	—
Coalsyn-impur	23.1489	34.7234	1.5774	—	—	—	21.4926	8.3802	9.2675	0.01	1	0.4

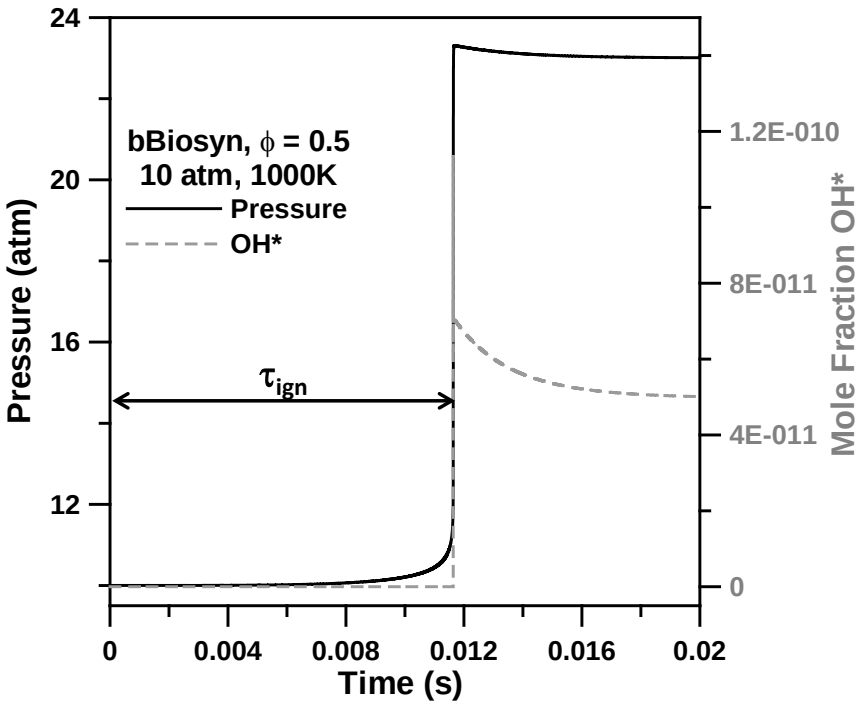

Fig. 4 Determination method for the ignition delay time using the computed pressure and OH* mole fraction profiles.

Model Validation. While the base C0-C3 mechanism has been validated against a large body of hydrogen and syngas data from the literature, it is however worth mentioning that there are very few experimental results available for syngas mixtures with impurities. To the best of the authors' knowledge, the only results available are the results from Mathieu et al. (2013a) where ignition delay times for baseline (H_2 and CO only) and realistic (H_2, CO, CO_2, CH_4, and H_2O) bio-syngas mixtures diluted in Ar, with and without NH_3, were measured at various pressures.

These results were computed with the detailed kinetics mechanism described above, and the results are visible in Fig. 5 for the baseline mixture and in Fig. 6 for the realistic mixture. As can be seen in Fig. 5, the model captures very well the experimental trends for all pressure conditions. Data at 30 atm were perfectly reproduced, and the lack of effect of NH_3 is captured. At 10 atm, ignition delay times are also perfectly reproduced by the model, except for the highest temperature when NH_3 is in the mixture, where a small discrepancy can be observed. While the model predicts a very small increase in the ignition delay time at this pressure when ammonia is added, it is difficult to observe such a small increase from the experimental results. At the lowest pressure investigated, the results are generally well reproduced except for the lowest temperatures where the model is under-reactive. The very small decrease in the ignition delay time observed when NH_3 is added, over most of the temperature range, can be observed both in the experiments and in the modeling at this pressure condition.

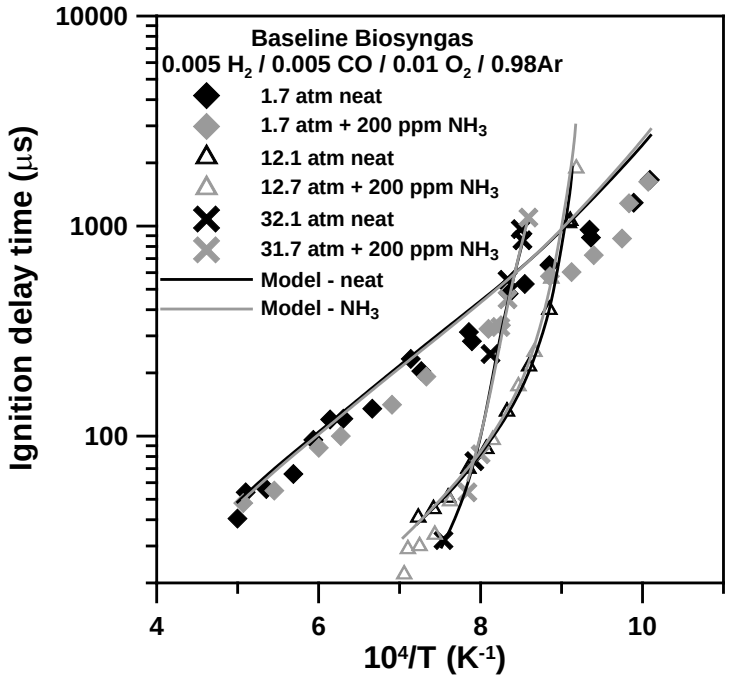

Fig. 5 Comparison between ignition delay times for a baseline (H_2/CO) biosyngas mixture diluted in Ar, with and without NH_3, from Mathieu et al. (2013a) and the model used in this study at various pressure conditions.

For the realistic biosyngas mixture, Fig. 6, the experimental trends associated with the pressure condition and the presence of NH_3 (very small increase in the ignition delay time for the latter case) are also captured by the model. However, for this type of mixture, the model tends to be under-reactive by a factor of around 2, especially on the low-temperatures side at 1.7 atm and on the high-temperatures side for higher pressures. This validation stage shows the ability of the model to reproduce experimental trends with good accuracy in the results. This comparison demonstrates the relevance of the mechanism used in this study to conduct a numerical investigation for the temperature and pressure range relevant to gas turbines.

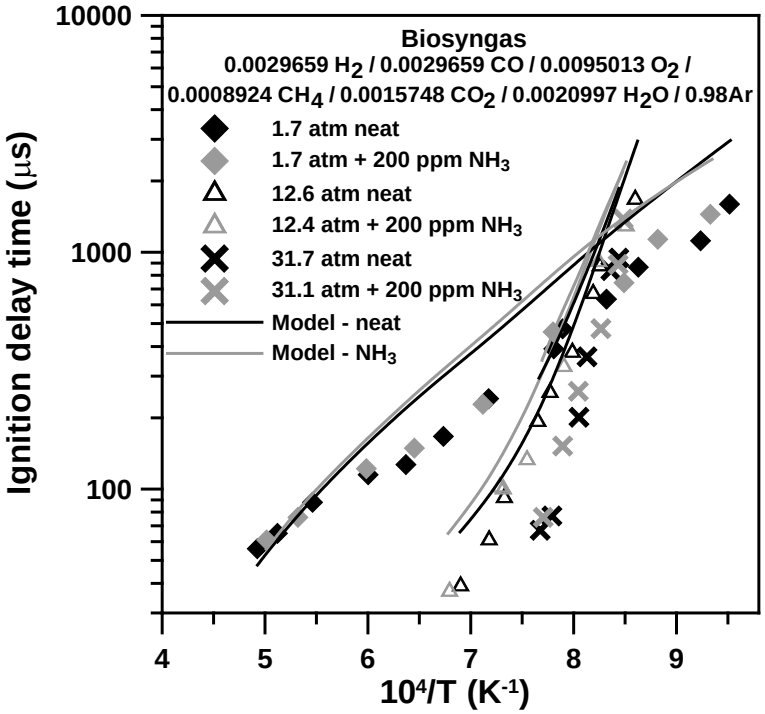

Fig. 6 Comparison between ignition delay times for a biosyngas mixture diluted in Ar, with and without NH_3, from Mathieu et al. (2013a) and the model used in this study at various pressure conditions.

Results. The results are presented as follows: first, the calculations for the neat baseline mixtures (CO and H_2 only) are covered to study the effect of the H_2/CO ratio. This series is followed by the effect of the impurity additions on these baseline mixtures. Finally, the averaged syngas mixtures including all species are considered with and without impurities. For each general category, the ignition delay time results are discussed first, followed by the laminar flame speed results.

Neat Baseline Mixtures. The effects of the ratio between CO and H_2 on the ignition delay time, for the three pressure conditions investigated, are typically small, as can be seen in Mathieu et al. (2013b). Therefore, the small change in the CO/H_2 ratio between the coal- and bio-syngases investigated herein does not really alter the predicted ignition delay times for these neat baseline mixtures; regardless of the temperature or pressure. One can mention that the main difference between these two syngases is that the ignition delay times are slightly shorter for the mixture that contains the higher proportion of H_2 (bio-syngas), but no change in the behavior was reported. One can also mention the important, and temperature-dependent, effect of pressure on the ignition delay time (see Mathieu et al. (2013b)). These effects were discussed in detail already [Kéromnès et al., 2013] and are essentially due to the competition between two reactions: the chain-branching reaction H + O_2 ⇄ OH + O (r1) and the chain-propagating reaction H + O_2 (+M) ⇄ HO_2 (+M) (r2). While r1 controls the reactivity at higher temperature, r2 is predominant at lower temperature. In addition, the transition from r2 to r1 is shifted to higher temperatures when the pressure is increased. This pressure dependence is due to the increased collisional

efficiency of r2 which decreases the overall reactivity. This reason explains why low-pressure experiments show a stronger reactivity than high-pressure experiments at the intermediate-temperature range.

Although the laminar flame speed for syngas mixtures was investigated for two temperatures and for two pressures, only two examples with the extreme conditions are discussed here. The trends and conclusions drawn from these two examples are indeed the same for the two other conditions, not shown. The difference between these two types of mixtures was discussed in detail previously [Mathieu et al., 2013b]. At 1 atm for an inlet temperature of 300 K with the baseline coal- and bio-syngases, the difference between the two types of syngas can be relatively important for this combustion property; the blend with the lowest amount of H_2 has the lowest flame speed, especially at fuel rich conditions. The difference between the two mixtures is close to 30 cm/s. Similar observations can be made for the 15-atm, 500-K condition, the difference being a little larger (45 cm/s). Note that the largest difference between the two syngases was observed for the 1 atm, 500-K case, which also corresponds to the condition where the flame speeds are the highest.

Impurity Addition to the Baseline Mixtures. The effects of impurity addition on the baseline bio-syngas mixture are visible in Figs. 7 (1 atm), 8 (10 atm), and 9 (35 atm). As can be seen in Fig. 7, only NO_2 seems to have an effect (promoting) on the ignition delay time, for temperatures lower than 1000 K. The differences in the ignition delay time induced by the presence of NH_3, HCN, or SO_2 are indeed too small to be discernible. At 900 K, the ignition delay time is reduced by about 85% by the addition of 400 ppm of NO_2, and this reduction in the ignition delay time reaches 92% for the highest NO_2 concentration investigated (bBiosyn-NO_2Hi mixture). The ignition delay times for the mixture containing all the impurities at their highest level are nearly the same as for the bBiosyn-NO_2Hi mixture, which indicates that there is no important interaction between the impurities at this condition.

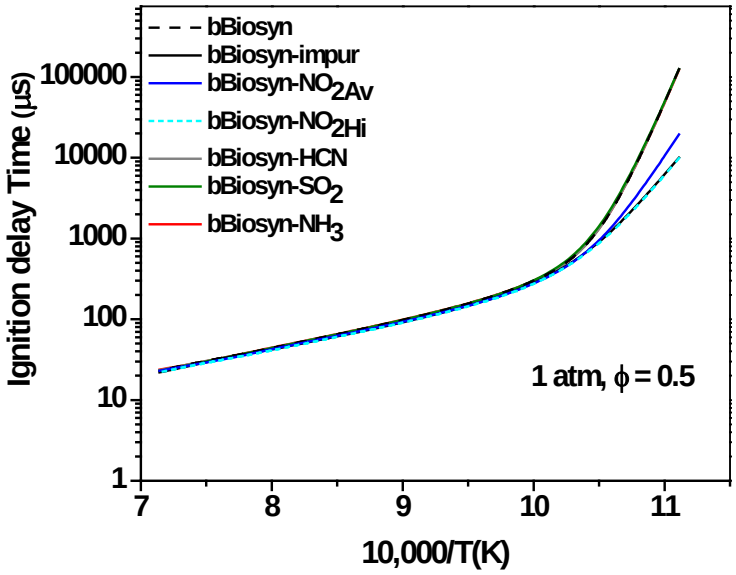

Fig. 7 Effect of various impurities on the ignition delay time for a baseline bio-syngas mixture at 1 atm.

At 10 atm (Fig. 8), similar to the atmospheric-pressure case, only NO_2 has an effect on the ignition delay time. This effect starts at higher temperatures, below 1150 K, and is less important than for the previous case: 23% and 45% reduction at 900 K for the bBiosyn-NO_2Av and bBiosyn-NO_2Hi mixtures, respectively.

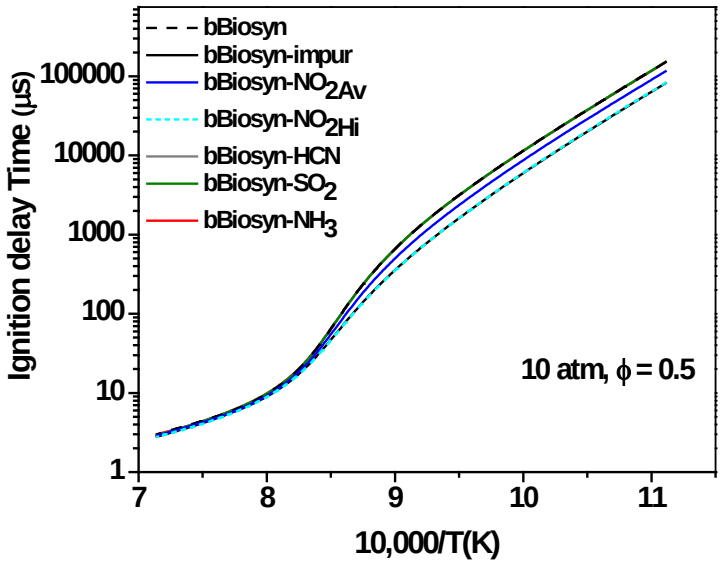

Fig. 8 Effect of various impurities on the ignition delay time for a baseline bio-syngas mixture at 10 atm.

A similar trend is followed at higher pressure, Fig. 9, where NO_2 has some effect at temperatures below 1250 K but with reductions in the ignition delay time that are less important: ignition delay times are shorter by around 19% with an addition of 400 ppm of NO_2 and by around 36% with 1200 ppm of NO_2 at 900K.

The effects on the ignition delay time of impurities that are more specific to coal syngas are visible in Figs. 10, 11, and 12 for pressures of 1, 10, and 35 atm, respectively. As can be seen in these figures, similar to the baseline bio-syngas, an addition of NH_3 does not modify the ignition delay time over the range of conditions investigated. A similar absence of any effect is observed with COS. However, if an averaged concentration of H_2S does not have a distinguishable effect on τ_{ign}, a relatively large concentration of this contaminant exhibits a large effect on the ignition delay time. At 1 atm (Fig. 10), it is visible that H_2S reduces the reactivity of the mixture over the entire range of temperature and strongly reduces the curvature of the neat mixture profile for temperatures below 1000 K. It is also worth mentioning that the mixture with all the impurities yields the same results as the bCoalsyn-H_2SHi mixture, indicating that there is no interaction between impurities at these conditions.

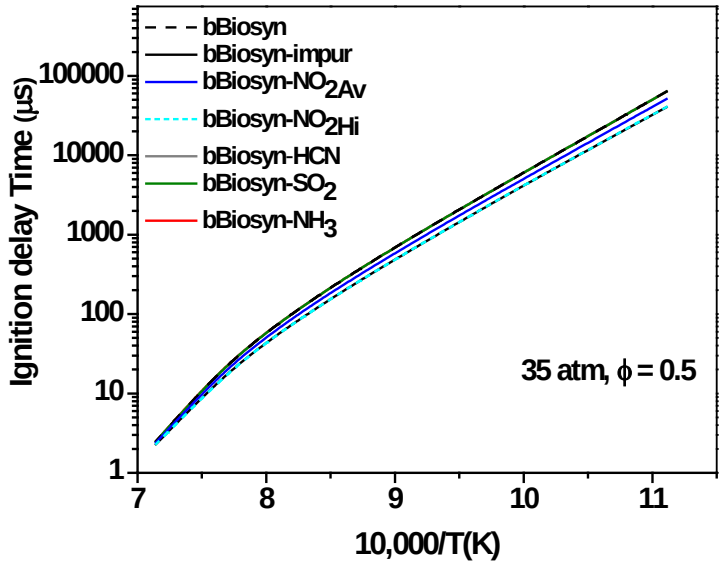

Fig. 9 Effect of various impurities on the ignition delay time for a baseline bio-syngas mixture at 35 atm.

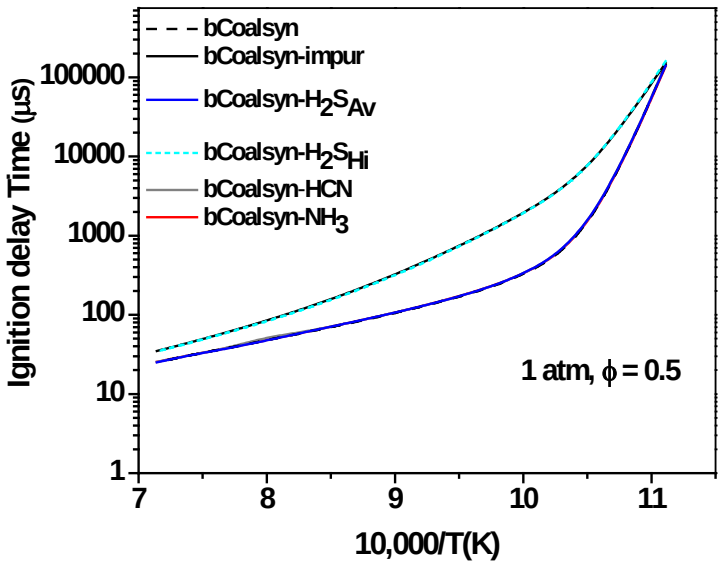

Fig. 10 Effect of various impurities on the ignition delay time for a baseline coal-syngas mixture at 1 atm.

At 10 atm, Fig. 11, the high concentration of H_2S is also the only case where an effect on the ignition delay time can be observed. Again, it seems that the curvature in τ_{ign} observed with the neat mixture is strongly reduced by the presence of this contaminate. In this case, however, the

reduction of the curvature corresponds to an increase in the ignition delay time for temperatures above 1150 K (by up to 46%) and to a decrease in τ_{ign}, as high as 60%, below this temperature.

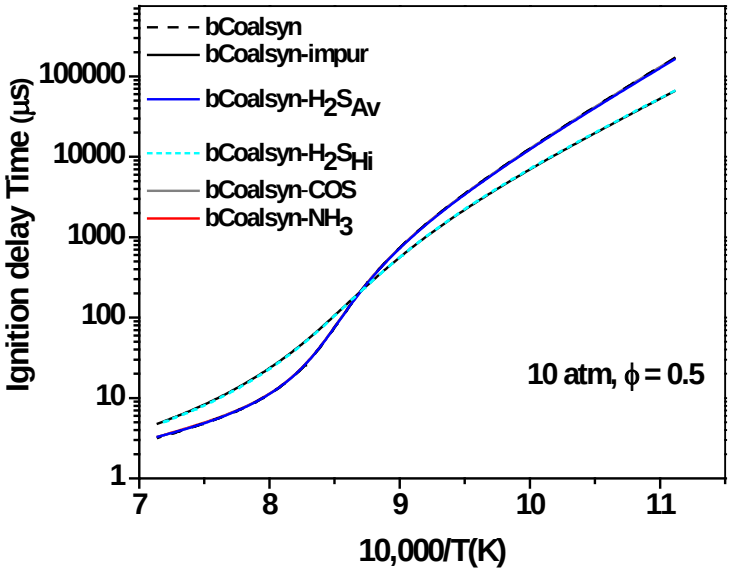

Fig. 11 Effect of various impurities on the ignition delay time for a baseline coal-syngas mixture at 10 atm.

At 35 atm, Fig. 12, the effects are similar to those observed at 10 atm but the temperature at which the curves cross is shifted to 1330 K. While the increase in τ_{ign} is rather moderate at the highest temperature investigated (from 3.2 to 4.8 μs), the increase in the reactivity due to the large H_2S concentration is rather important on the low-temperature side (from 168,500 to 65,000 μs).

The effect of the equivalence ratio was also investigated in this study. Since this effect has been studied already by the authors [Mathieu et al., 2013b] with neat mixtures. To summarize these results, increasing the equivalence ratio from 0.5 to 1.0 has nearly no effect on the ignition delay time at 1 atm for the bBiosyn mixture. A small decrease in the reactivity is observed at the two temperature extremities at 10 atm (4.5% difference at the highest temperature and up to 13.7% for the lowest temperature), while the decrease in the reactivity covered most of the temperature range at 35 atm. Similar results were observed for the bCoalsyn mixture.

In the presence of impurities, Fig. 13, the ignition delay times of a baseline bio-syngas mixture doped with impurities seem to be modified in larger proportion by a change in the equivalence ratio than for the neat mixture. The ignition delay time is indeed decreased by between 20% (1400 K) and 45% (900 K) at 1 atm and up to 55% at 10 atm, 900 K. For the highest pressure investigated, the reduction in τ_{ign} is between 25% at 1400 K and 50% at 900 K.

Concerning the baseline coal-syngas mixture with impurities, Fig. 14, the effect of the equivalence ratio on τ_{ign} seems a bit more complex. Indeed, the ignition delay time is slightly increased at 1 atm for temperatures above 950 K and is decreased below this temperature. It is also worth mentioning that a similar behavior is observed at 10 atm, with the pivot temperature being around 1135 K. At 35 atm, τ_{ign} are shorter for the highest equivalence ratio over the entire range of temperature investigated, the decrease being very small at high temperature and above 35 % at 900 K.

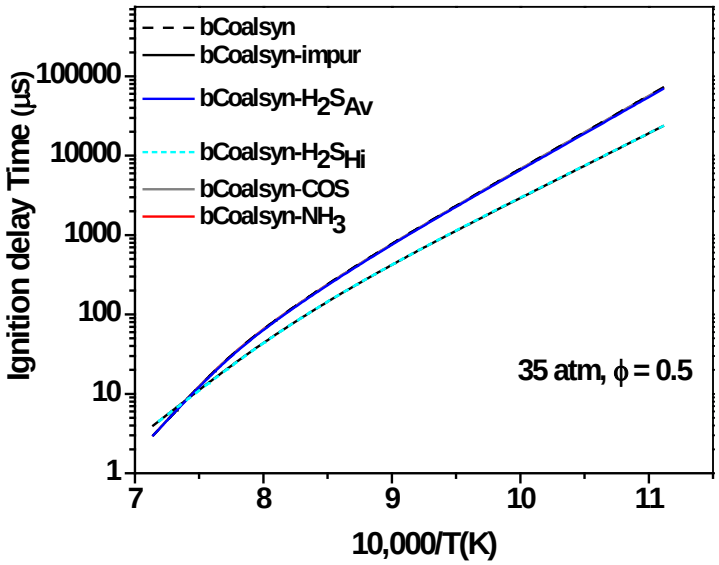

Fig. 12 Effect of various impurities on the ignition delay time for a baseline coal-syngas mixture at 35 atm.

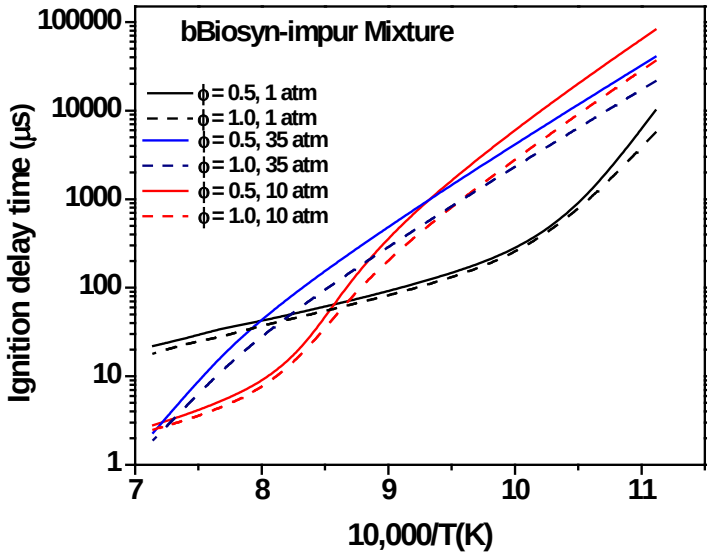

Fig. 13 Equivalence ratio effect on the ignition delay time for a baseline bio-syngas mixture with impurities at 1, 10, and 35 atm.

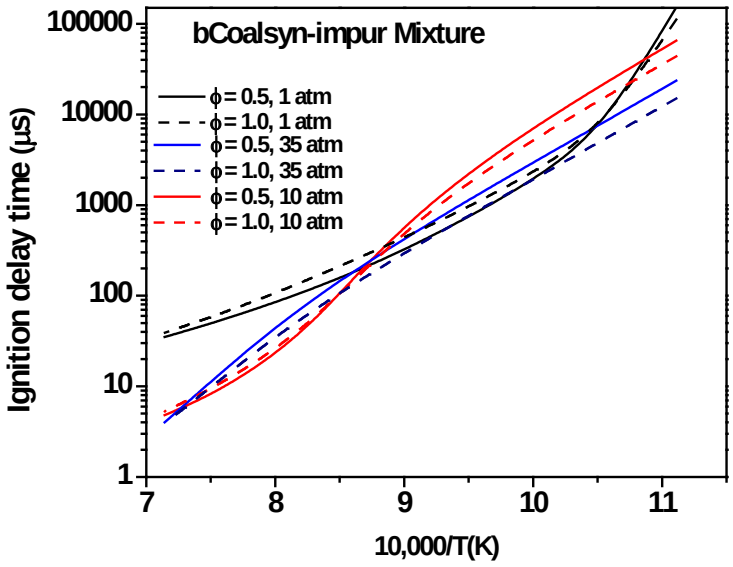

Fig. 14 Equivalence ratio effect on the ignition delay time for a baseline coal-syngas mixture with impurities at 1, 10, and 35 atm.

It is interesting to compare the effects of hydrocarbon addition, investigated in Mathieu et al. (2013b), with the effects of impurity addition on the baseline syngas mixtures investigated herein. As can be seen in Fig. 15 for the bBiosyn mixture, the effects from hydrocarbon addition are overall higher than the effects for impurity addition. This is particularly true at 1 atm where a large effect of hydrocarbon addition is visible on the entire range of conditions against the low-temperature side only for the impurities. At 10 atm, it is interesting to see that the effects of hydrocarbons are visible only on the high-temperature side, whereas the impurity effect is still observed for low temperatures at this pressure condition. The same behavior is observed for the 35-atm case, although the effects of both hydrocarbons and impurities are smaller at this pressure condition. Similar observations can be made for the coal-syngas mixture, Fig. 16, although the hydrocarbon-addition effects are less important in this case.

The effects on the laminar flame speed of various impurities with bBiosyn at 1 atm, 300 K and 15 atm, 500 K as initial conditions are visible in Fig. 17 and Fig. 18, respectively. As can be seen in Fig. 17, the addition of impurities has a small effect on the laminar flame speed and this effect is visible for fuel rich conditions only, for an equivalence ratio larger than 1.5. Results are also somewhat contrary to what has been observed for the ignition delay time: the reactivity of the mixture is decreased by the impurity addition and this effect is found for all the impurities except NO_2 and SO_2. The largest effect is provided by NH_3 (reduction of the maximum S_L by 5cm/s), and the maximum laminar flame speed is only reduced by a few cm/s, from 191 to 189 cm/s, for the 0.28% NH_3 addition. When all the impurities are added together, the laminar flame speed is further reduced. However, the reduction corresponds to the sum of the effects from NH_3 and HCN, indicating that there is no enhancing or inhibiting interaction between these impurities.

At the other extreme condition, 500 K and 15 atm (Fig. 18), laminar flame speeds are higher but trends in the results are similar. However, the decrease in the laminar flame speed with impurities is slightly larger, from 271 to 258 cm/s, with NH_3.

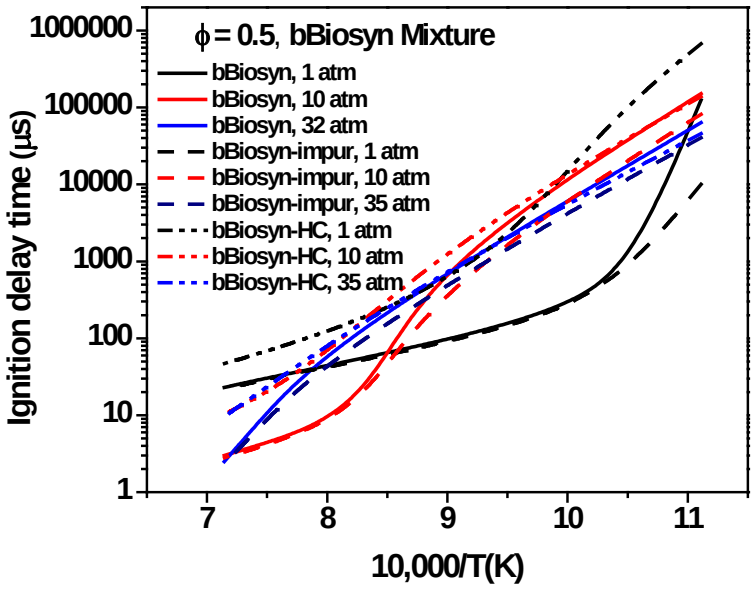

Fig. 15 Impurity- and hydrocarbon-addition effects on the ignition delay time of a baseline bio-syngas mixture at ϕ = 0.5 and at 1, 10, and 35 atm.

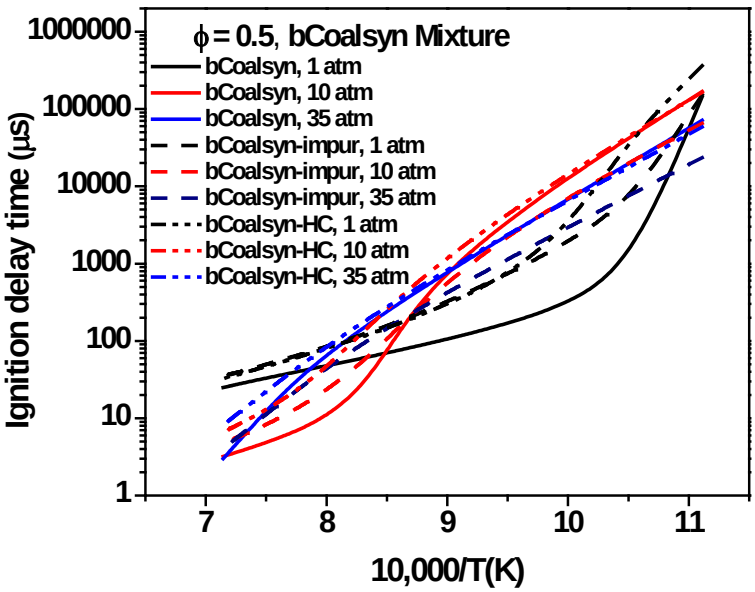

Fig. 16 Impurity- and hydrocarbon-addition effects on the ignition delay time of a baseline coal-syngas mixture at ϕ = 0.5 and at 1, 10, and 35 atm.

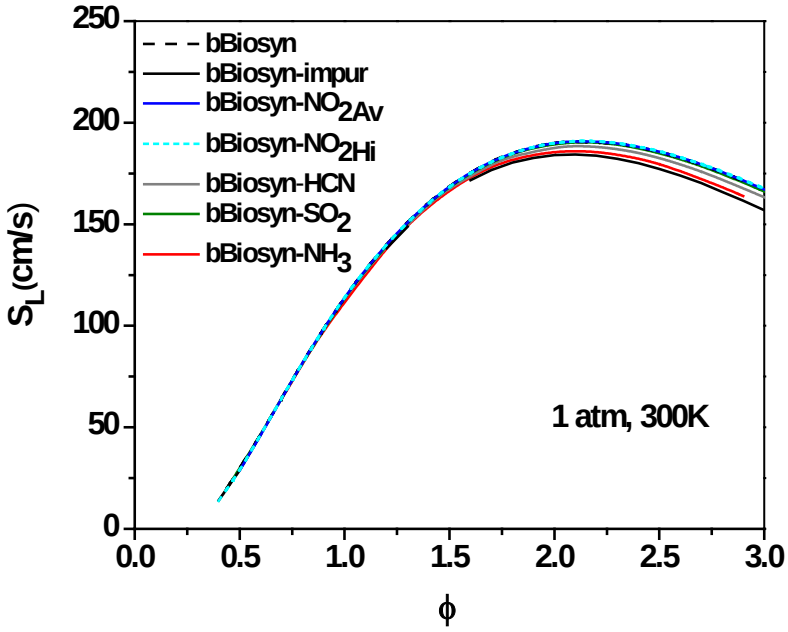

Fig. 17 Laminar flame speed as a function of equivalence ratio for a baseline bio syngas with various impurities and at 1 atm and 300 K as initial conditions.

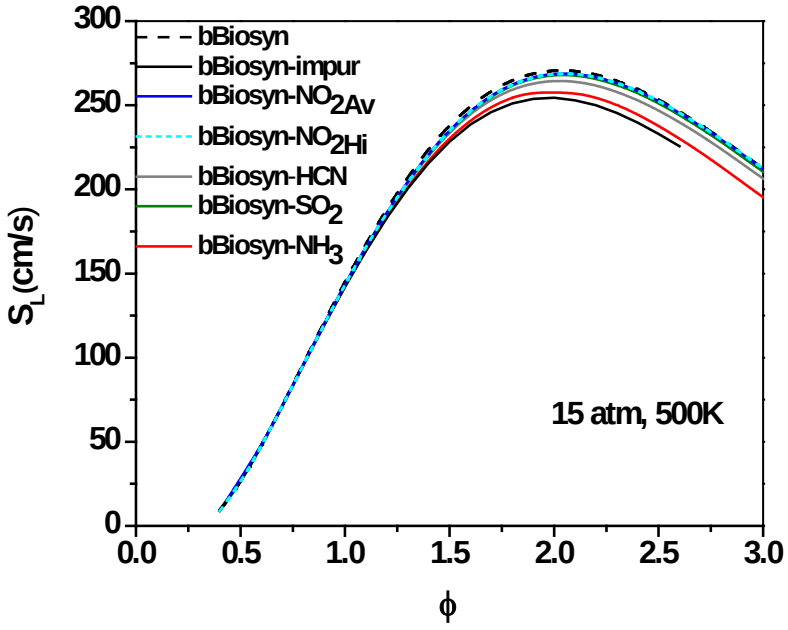

Fig. 18 Laminar flame speed as a function of equivalence ratio for a baseline bio syngas with various impurities and at 15 atm and 500 K as initial conditions.

For the bCoalsyn mixture, Fig. 19, a decrease in the laminar flame speed is still observed with the NH_3 addition. A low concentration of H_2S seems to be without effect, while a relatively large reduction of the laminar flame speed (from 169 to 153 cm/s for the maximum flame speed) can be observed with the highest H_2S concentration. As for the bBiosyn mixtures, these effects are observed for equivalence ratios above 1.5 only and the effects of impurities on the laminar flame speed (NH_3 and H_2S in this case) seem to add to each other without apparent interaction.

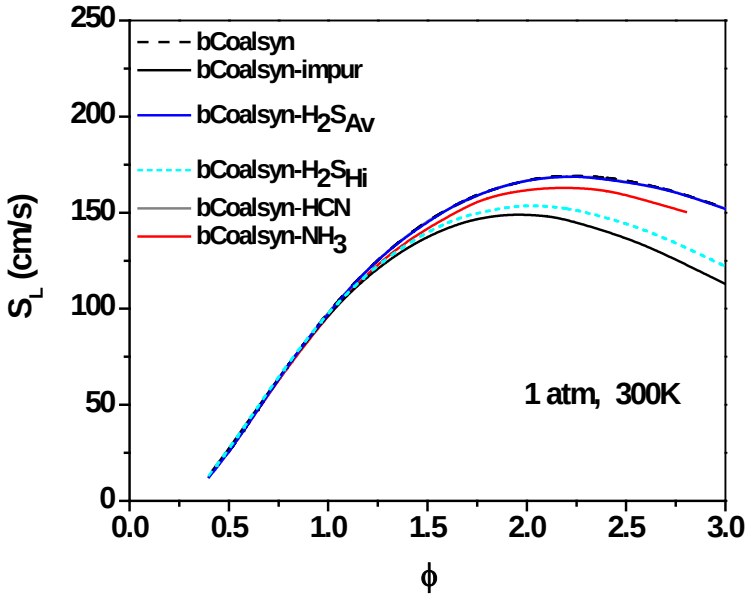

Fig. 19 Laminar flame speed as a function of equivalence ratio for a baseline coal syngas with various impurities at 1 atm and 300 K as initial conditions.

Figure 20 shows the results at the other extreme conditions, 500 K and 15 atm. As can be seen, the trends are the same as for the 300-K, 1-atm case. However, one can notice the higher flame speed at this condition and the fact that the maximum flame speed is shifted towards lower equivalence ratios. The effect of impurities is also slightly higher at this extreme condition and this result seems to be mostly due to the pressure increase (by comparing results obtained at 15 atm, 300 K and 1 atm, 500 K, not shown).

The influence of impurity addition on the baseline biosyngas can be compared to the effects of hydrocarbon addition at 1 atm and 300 K in Fig. 21. It is visible in this figure that the effect of impurities is significantly smaller than the effect of hydrocarbons. Indeed, while the impurities decreased the laminar flame speed by only about 3%, S_L is reduced by 55% when hydrocarbons are present, and the equivalence ratio for which this maximum in the flame speed is observed is also notably decreased, from 2.1 to 1.3.

At higher pressure and temperature, Fig. 22, the difference between impurities and hydrocarbon addition is even higher: a 66% decrease in S_L was observed for the hydrocarbon addition (with a maximum in S_L observed at ϕ = 2.0 for the baseline and 1.2 or the hydrocarbon addition) and around 6% for the impurities.

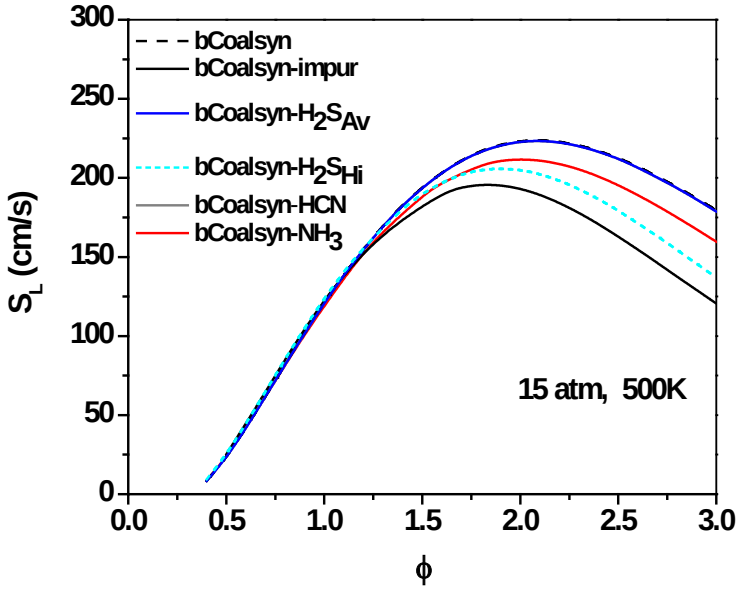

Fig. 20 Laminar flame speed as a function of equivalence ratio for a baseline coal syngas with various impurities and at 15 atm and 500 K as initial conditions.

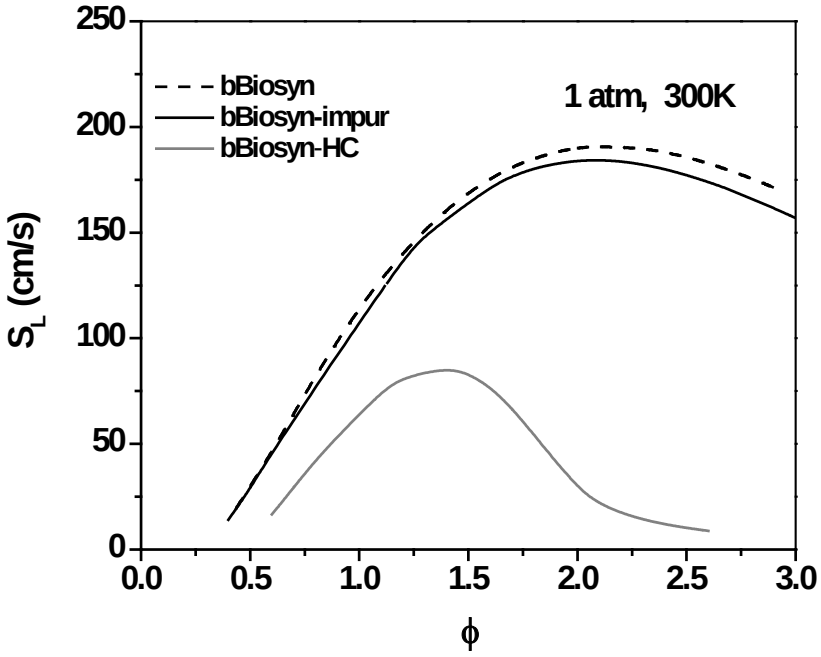

Fig. 21 Laminar flame speed as a function of equivalence ratio for a baseline bio syngas with various impurities or hydrocarbons at 1 atm and 300 K as initial conditions.

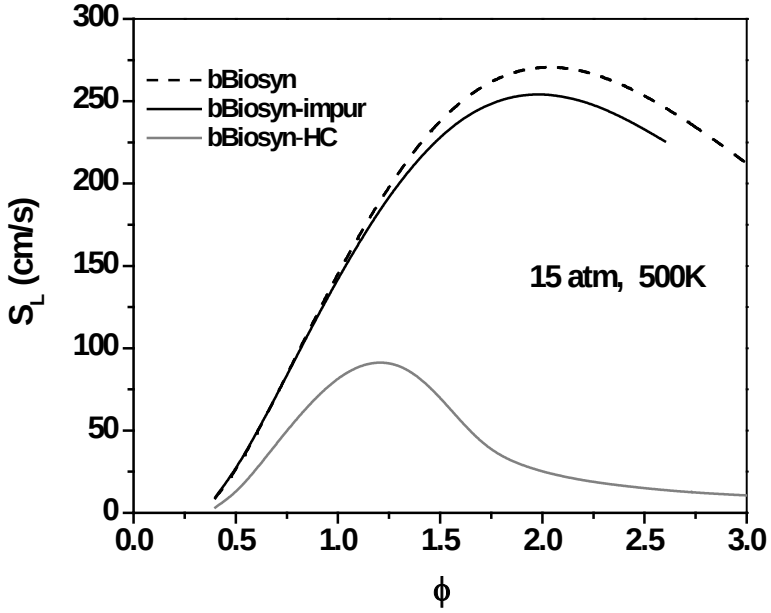

Fig. 22 Laminar flame speed as a function of equivalence ratio for a baseline bio-syngas with various impurities or hydrocarbons at 15 atm and 500 K as initial conditions.

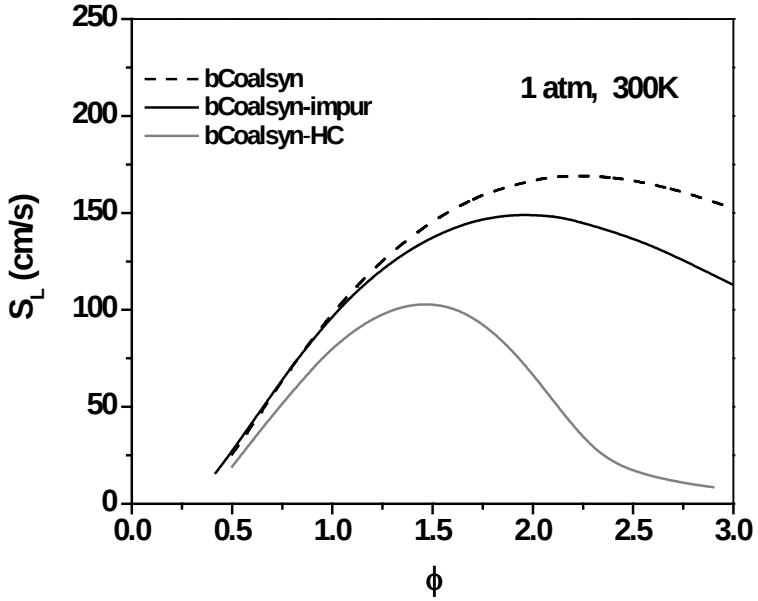

Fig. 23 Laminar flame speed as a function of equivalence ratio for a baseline coal syngas with various impurities or hydrocarbons at 1 atm and 300 K as initial conditions.

The same comparison between the effects of impurities and hydrocarbons was made for the baseline coal syngas at 1 atm, 300 K (Fig. 23) and 500 K, 15 atm (Fig. 24). One can notice from these figures that the effects of impurities are more important for the coal syngas than for the bio-syngas while the effects of the hydrocarbons are lower. As a result, while a significant difference can be observed between these two kinds of addition, the difference is not as large as for the bio-syngas (S_L reduction of 12% by impurities and 39% by hydrocarbons at 300 K and 1 atm and of 13% and 51%, respectively, for the 500-K, 15-atm condition).

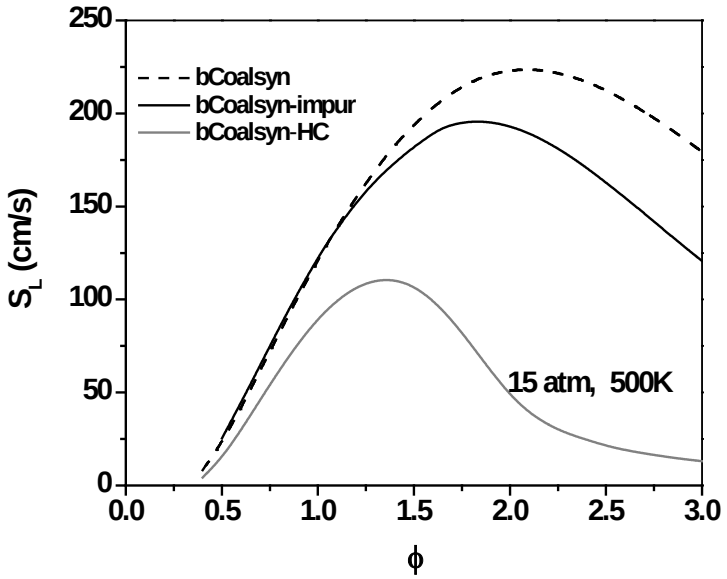

Fig. 24 Laminar flame speed as a function of equivalence ratio for a baseline coal syngas with various impurities or hydrocarbons at 15 atm and 500 K as initial conditions.

Impurity Addition to the Average Mixture. A comparison between the ignition delay times of the two averaged mixtures (from coal and biomass) for the three pressure conditions investigated has been made in Mathieu et al. (2013b). Some significant differences between these two mixtures were observed due to the difference in hydrocarbon composition. The equivalence ratio effect for the two average mixtures is visible in the authors' previous work [Mathieu et al., 2013b].

The effects of impurity addition on the ignition delay time of the average bio-syngas mixture at 1 atm are visible in Fig. 25. It is visible from this figure that, as for the baseline mixtures, only NO_2 has an effect on the ignition delay time. Indeed, ignition delay times are notably decreased below 1000 K in the presence of NO_2; the amplitude of this decrease being proportional to the concentration of NO_2 at the authors' conditions. The ignition delay times for the mixture with all the impurities are similar to the ones from the high NO_2 concentration mixture, indicating a lack of effect of NH_3, HCN, and SO_2.

At 10 atm, Fig. 26, the trends are similar to those described at 1 atm (decrease of the ignition delay time on the low-temperature side, for NO_2 only). The decrease in the ignition delay time was relatively small and was observed only for temperatures below 1250 K.

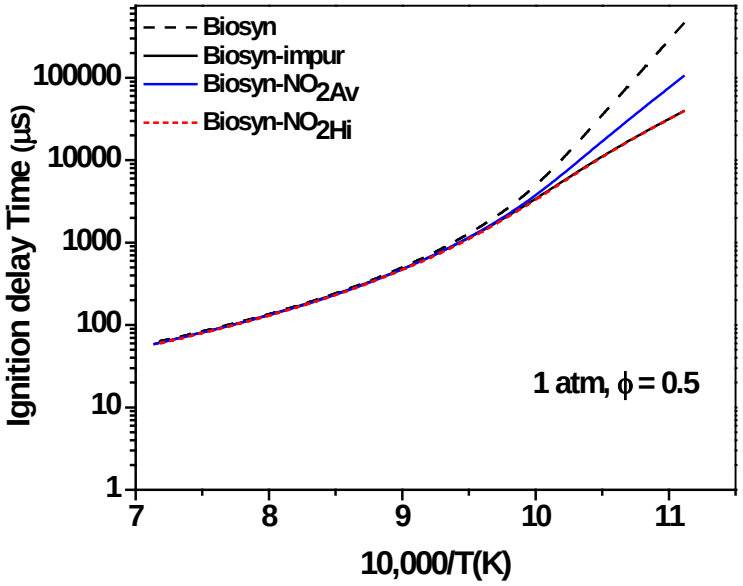

Fig. 25 Effect of various impurities on the ignition delay time for an average bio-syngas mixture at 1 atm.

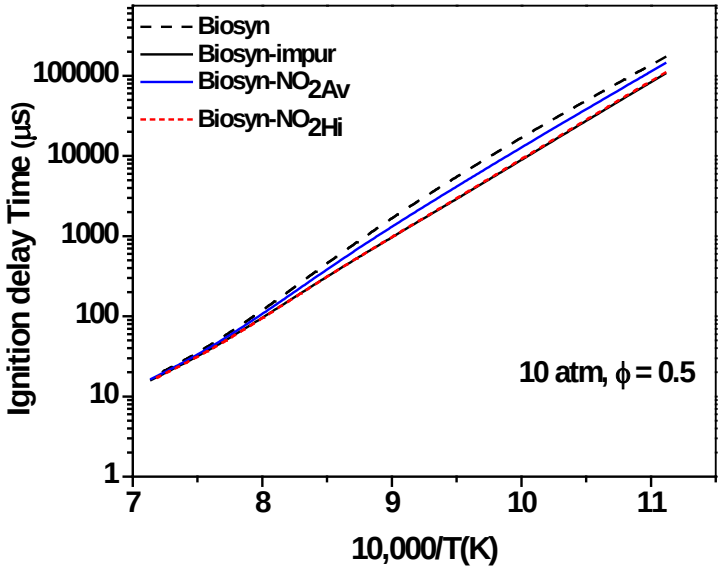

Fig. 26 Effect of various impurities on the ignition delay time for an average bio-syngas mixture at 10 atm.

As can be seen for the case at 35 atm in Fig. 27, effects of impurities on the ignition delay time are relatively small at these conditions. Again, only NO_2 has an effect (enhancing reactivity) on the ignition delay time. This effect is however distributed nearly equally along the range of temperatures investigated.

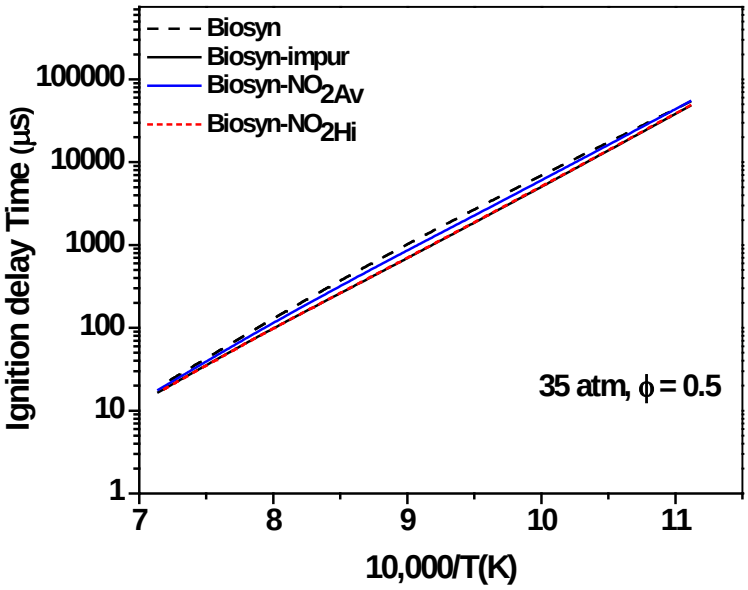

Fig. 27 Effect of various impurities on the ignition delay time for an average bio-syngas mixture at 35 atm.

The effects of impurities on the Coalsyn mixture at 1 atm are visible in Fig 28. As can be seen, the average concentration of H_2S has no effect on the ignition delay time at this condition. The ignition delay time is however notably increased for temperatures above 975 K by a factor between 2 (1400 K) and 5 (1050 K) for the highest H_2S concentration. The calculations yield the same result for the Coalsyn-impur mixture, indicating that the other impurities have no effect overall.

At 10 (Fig. 29) and 35 atm (Fig. 30), the results obtained with the lowest concentration of H_2S investigated are without effect. However, a noticeable effect on the ignition delay time is exhibited by the high H_2S concentration and, again, no further effect is seen with all impurities. At 10 atm, the H_2S addition decreases the ignition delay time below 1225 K and increases it above this temperature. At 35 atm, ignition delay times are not changed by the impurity addition at 1400 K. However, below this temperature, a noticeable decrease can be observed with the highest H_2S concentration, this decrease being larger as the temperature decreases.

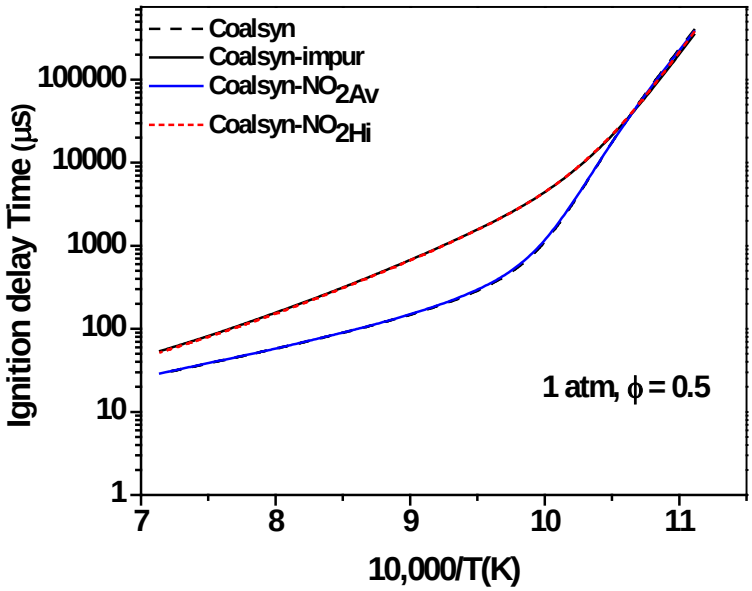

Fig. 28 Effect of various impurities on the ignition delay time for an average coal-syngas mixture at 1 atm.

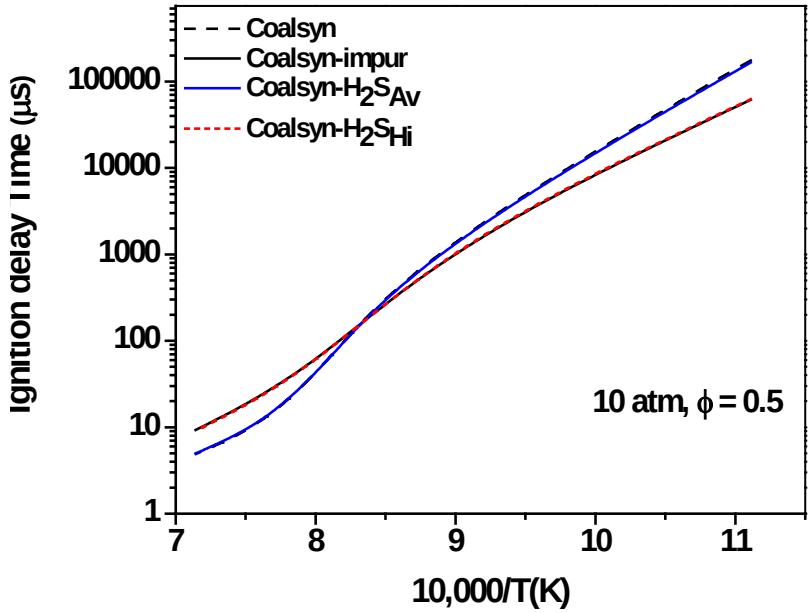

Fig. 29 Effect of various impurities on the ignition delay time for an average coal-syngas mixture at 10 atm.

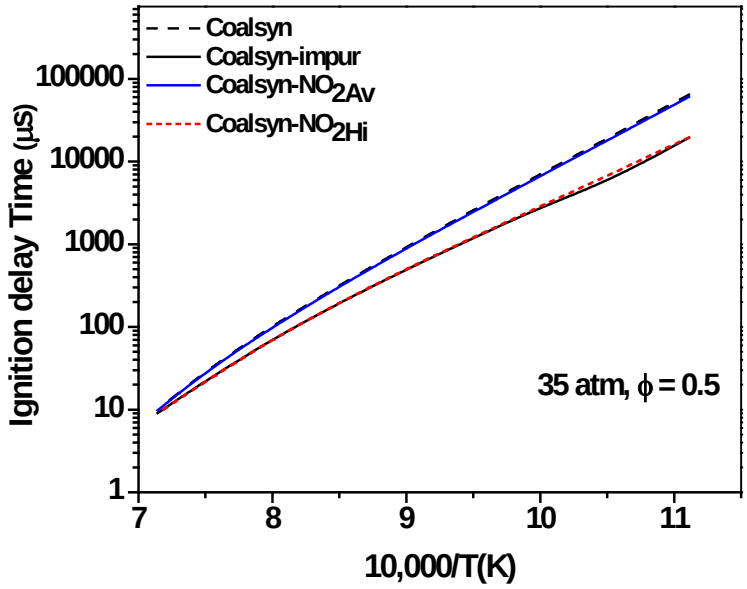

Fig. 30 Effect of various impurities on the ignition delay time for an average coal-syngas mixture at 35 atm.

The effects of impurities on the laminar flame speed of an average coal syngas mixture, with initial conditions of 1 atm and 500 K, are visible in Fig. 31. As can be seen, the smallest H_2S concentration investigated does not exhibit any effect on S_L. A noticeable decrease (around 5%) in the laminar flame speed is however observed with the high H_2S concentration for fuel rich conditions. The laminar flame speed is further reduced (by around 9% total) when all the impurities are in the mixture.

At higher pressure, Fig. 32, laminar flame speeds are significantly smaller, with a reduction higher than 50% due to the initial pressure increase. Impurity effects are the same as for the low-pressure case, and the percentage reduction in the maximum laminar flame speed is also the same as for the previous case with lower initial pressure.

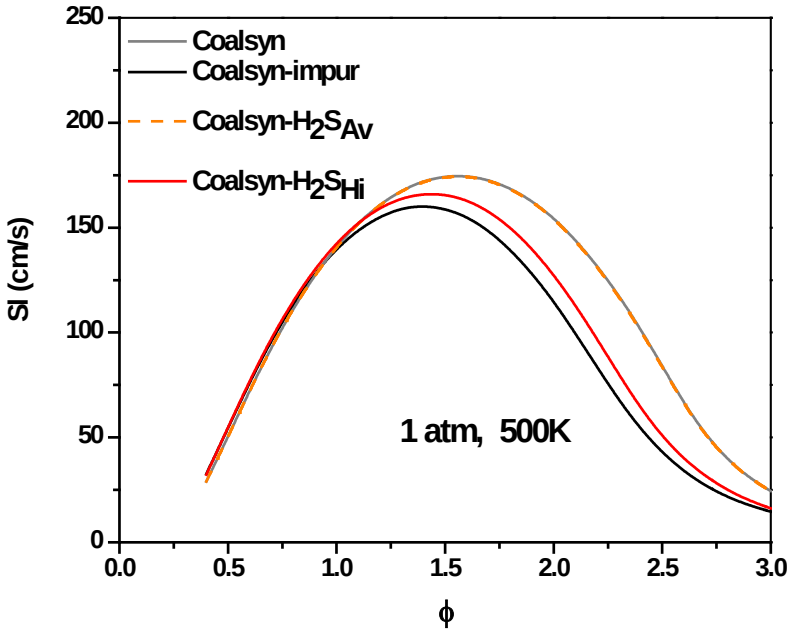

Fig. 31 Effect of various impurities on the laminar flame speed for an average coal-syngas mixture at 1 atm, 500 K as initial conditions.

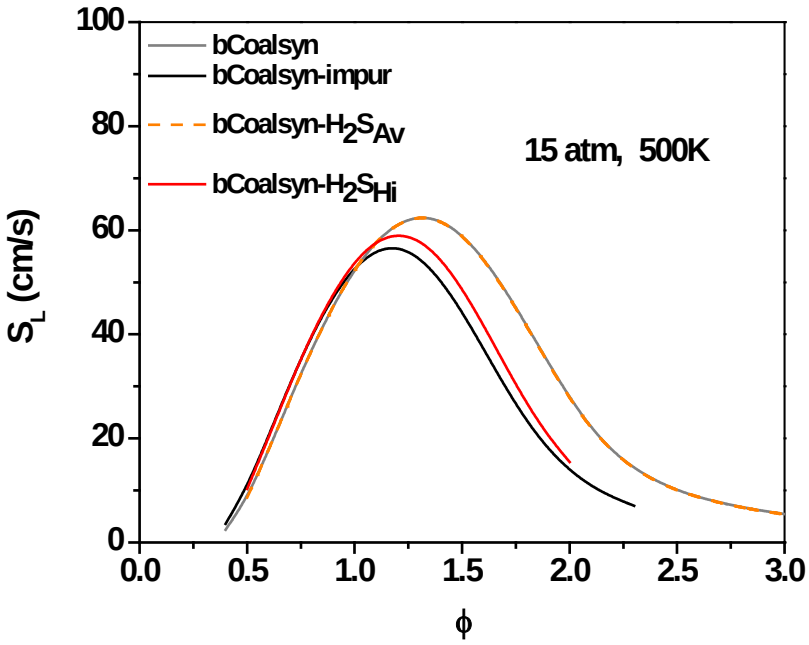

Fig. 32 Effect of various impurities on the laminar flame speed for an average coal-syngas mixture at 15 atm, 500 K as initial conditions.

Discussion. For the bio-syngas mixtures, the results showed that NO_2 was the only impurity to have an effect on the ignition delay time. This effect is present only when the low-temperature chemistry of H_2 rules the combustion (i.e. when the HO_2 radical dominates over OH). This behavior indicates a purely chemical mechanism due to the reaction $NO + HO_2 \rightleftarrows NO_2 + OH$ (r3) (NO_2 being mostly converted to NO by the reaction $NO_2 + H \rightleftarrows NO + OH$ (r4)). The OH radicals produced then oxidize the hydrogen via $OH + H_2 \rightleftarrows H_2O + H$ (r5), and this reaction then allows recycling NO via r4. This catalytic effect of NO_2 which transforms HO_2 into OH explains the large effects observed on the ignition delay time, when the low-temperature chemistry was dominating. The lack of effect of NO_2 on the flame speed, where the high-temperature chemistry of H_2 dominates, associated with the unmodified flame temperature, confirms the chemical role of NO_2.

For the coal baseline syngas, H_2S is the only contaminant that has an influence on the ignition delay time. An effect on the laminar flame speed was observed too, with the highest impurity concentration studied. The inhibiting effect occurring at high temperature or with the laminar flame speed is due to the reaction $H_2S + H \rightleftarrows SH + H_2$, (r6) which occurs before the ignition and inhibits the dominating reaction $H + O_2 \rightleftarrows OH + O$ (r1) and reduces the overall reactivity of the mixture. The H_2S can therefore be viewed as a sink for H radicals, preventing r1 to take place and to trigger the ignition. The absence of change in the flame temperature, even for the highest H_2S concentration investigated, indicates a purely chemical effect of H_2S on the laminar flame speed. At this condition, the high-temperature mechanism via r6 is responsible for the decrease in the mixture's reactivity. For the conditions where H_2S is promoting the reactivity on the ignition delay time, this result can be explained by the fact that H_2S reacts with radicals (H, O, OH, and HO_2) to give SH + products, and this radical consumption limits the important reactions for H_2 oxidation, namely $H + O_2 \rightleftarrows OH + O$ (r1) and $H + O_2 + M \rightleftarrows HO_2 + M$ (r2), the latter being more important at these conditions. Most of the SH will then either quickly form SO which will then form SO_2 via the reaction $SO + O_2 \rightleftarrows SO_2 + O$ or react through $SH + SH \rightleftarrows H_2S + S$ (r7). The S produced will then react through $S + O_2 \rightleftarrows SO + O$ (r8) and $SO + O_2 \rightleftarrows SO_2 + O$ (r9).

To summarize, at conditions where r2 dominates, the formation of HO_2 is limited by the presence of H_2S via the consumption of H radicals (r6) whereas the SH produced will then lead to the formation of O radicals via r8 and r9. These O radicals will then react through $O + H_2 \rightleftarrows OH + H$ (r10) and, overall, promote the reactivity of the mixture compared to the conditions where r2 was dominant, without H_2S.

Although NH_3 and HCN did not exhibit any effect on the ignition delay time, these components reduced the flame speeds for the baseline mixtures, mostly on the fuel rich side. These inhibiting effects are purely chemical effects as the laminar flame temperature is nearly unchanged by the presence of these components. This result is visible for the NH_3 case in Fig. 34, where all the adiabatic flame temperatures are the same for a given equivalence ratio, regardless of the nature or concentration of the contaminants. Note that this outcome is also true for the other conditions investigated, including the baseline coal mixture. The chemical analysis showed that this inhibiting effect is chiefly due to the consumption of OH radicals, leading to water and a less-reactive radical (such as NH_2 for NH_3 or SH for H_2S). Overall, the reactive OH radicals are then replaced by less-reactive ones, slowing down the reactivity. This effect is particularly visible at

fuel rich conditions, where there is already a shortage of oxygen to complete the combustion of all the fuel molecules.

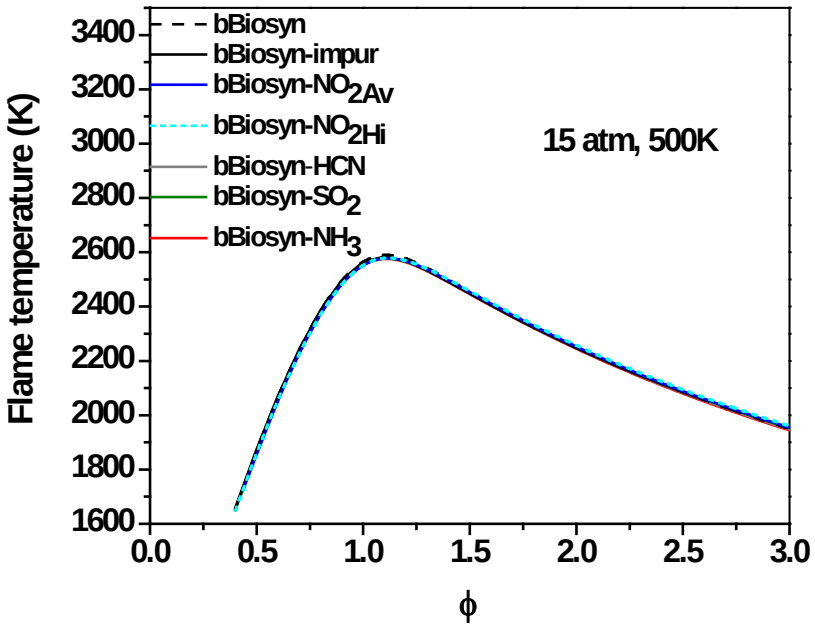

Fig. 34 Effect of various impurities on the adiabatic flame temperature for an average bio-syngas mixture at 15 atm, 500K as initial conditions.

Laminar Flame Speeds with Hydrocarbon Impurities

Synthetic gas, or syngas, is a mixture primarily composed of CO and H_2. This high-hydrogen combination causes it to be an attractive fuel for power generation through gas turbines. However, the concentrations of each species will vary depending on the feedstock and the process used to gasify it. In the ideal case, the syngas mixture would just consist of CO and H_2, but rarely is the mixture this simple. As the composition of syngas can vary greatly, it is important to look at all possible and likely impurities individually to fully understand their effects. This approach will allow gas turbine manufactures the freedom to design safe and efficient turbines that can operate with a variety of syngas mixtures.

Previous studies have shown that there are several impurities that can be present in typical syngas blends. A recent detailed study by the authors focused on the effects of nitrogen- and sulfur-based impurities [Mathieu et al., 2014a]. A detailed review of all previous studies of syngas mixtures can be found in Lee et al. (2014). However, the individual effects of small hydrocarbons, commonly found in syngas mixtures have not been well studied experimentally with respect to fundamental combustion parameters such as laminar flame speed and ignition delay time. The recent modeling study by Mathieu et al. (2014a) built upon their results presented previously [Mathieu et al., 2014b], where the previous work had looked specifically at the effects of hydrocarbon addition to syngas for fuel-air mixtures at engine conditions from a numerical perspective. They found that realistic levels of smaller hydrocarbons present in the syngas fuel blend, up to about 15% by volume, can significantly decrease the laminar flame speed by as much as a factor of two in some cases. The current study builds on the flame speed and ignition delay time modeling research of Mathieu et al. (2014a) to gain an experimental understanding of the effects of hydrocarbon impurities on the flame speed of syngas mixtures and to help validate the chemical kinetics mechanism. The present study therefore focuses on the hydrocarbons shown in Mathieu et al. (2014a) to be present in the largest concentrations and to have the greatest impact on the flame speed, namely methane and ethane.

Presented in this section of Task 3 are the results of new experiments for syngas-based laminar flames speeds with and without hydrocarbon impurities along with the results of a modern chemical kinetics model. The mixture compositions of interest herein are covered first, followed by details of the experimental setup and procedure. Details on the experimental results and a comparison of them to the predictions of the kinetics model are then given. Some discussion on the thermal-diffusive nature of the flames for the various blends as well as an analysis of the chemical kinetics are also provided in a discussion section.

Mixtures Investigated. As mentioned above, the mixtures chosen in this study were based off of an earlier numerical studies done by the authors' groups [Mathieu et al., 2014a; 2014b]. This prior study included two baseline syngas mixtures. These blends were chosen to represent a nominal Coal syngas and a nominal Bio-syngas fuels. The Coal syngas has a 60/40 ratio of CO to H_2, while the Bio-syngas has a 50/50 ratio. Hydrocarbons were then added to each mixture while holding the ratio of CO to H_2 constant. The hydrocarbons chosen for further study were the ones predicted to have the most-significant impact on the laminar flame speed. A detailed breakdown of the resulting mixtures tested in the present study is shown in Table 3.

As seen in Table 3, the two hydrocarbons investigated in this study were methane and ethane. Methane was found to have the greatest presence in the syngas mixtures, reaching 15% for bio-syngas and 7.4% for the coal-derived syngas. Model predictions showed that this large percentage of methane would have a significant impact on the flame speed [Mathieu et al., 2014b]. Ethane was chosen not because it comprised a large percentage of the fuel, 0.8% for bio-syngas and 1.7% for coal syngas, but because of the significant reduction in flame speed prediction that the small percentage of ethane was predicted to cause.

Table 1 Syngas mixtures with HC impurities.

Mixtures Investigated (Mole Fraction)				
Mixture	H_2	CO	CH_4	C_2H_6
Coal-Neat	0.400	0.600	--	--
Coal-1.6% CH_4	0.3936	0.5904	0.016	--
Coal - 7.4% CH_4	0.3704	0.5556	0.074	--
Coal – 1.7% C_2H_6	0.3932	0.5898	--	0.017
Bio-Neat	0.500	0.500	--	--
Bio-5% CH_4	0.475	0.475	0.050	--
Bio-15% CH_4	0.425	0.425	0.150	--
Bio-0.8% C_2H_6	0.496	0.496	--	0.008

This study investigated the high and low extremes of methane found to be present in syngas mixtures. For the coal syngas, the two levels of methane investigated were 1.6% and 7.4% of the fuel by volume. The bio-syngas added methane at 5% and 15%. Ethane was added to both syngas mixtures, with a percentage of 1.7% of the fuel for the coal syngas and 0.8% for the Bio-syngas.

Experimental Setup. Experiments were conducted in the high-pressure, high-temperature, stainless steel, constant-volume bomb at Texas A&M University. The design of this vessel is explained in detail in Krejci et al. (2013). The internal dimensions of the vessel are a 31.8 cm diameter and a length of 28 cm. Flames can be measured under near-constant-pressure conditions to a diameter of 12.7 cm.

All mixtures were made using the partial pressure method via a 0-1000 Torr pressure Transducer, and the experiments were conducted at room temperature (296 K ± 2 K). Research grade (99.5% pure) Methane, Ethane, Hydrogen, Carbon Monoxide as well as ultra-high purity (99.999%) Oxygen and Nitrogen were used. For the low-Methane coal syngas and the Ethane mixtures, the respective hydrocarbon and Hydrogen were premixed in a separate mix tank prior to being added to the vessel. All other components were added individually.

Each gaseous mixture was ignited by a central spark ignition system. Experimental data were collected using a high-speed camera (Photron Fastcam SA1.1) and a Z-type schlieren setup. The frame rate of the camera was adjusted as necessary to capture enough frames to successfully analyze each experiment. Frame rates used for this data set ranged from 3,000 to 18,000 fps. Images were processed using an internally developed MATLAB-based edge detection program. The unburned, unstretched flame speed and burned-gas Markstein length were calculated using

the appropriate nonlinear method as outlined by Chen (2010). The overall average uncertainty in the measured flame speed herein is estimated to be ± 7.2 cm/s.

Chemical Kinetic Model. The laminar flame speeds in this work have been simulated using AramcoMech 1.3 [Metcalfe et al., 2013], which was developed to describe the oxidation of small hydrocarbon and oxygenated hydrocarbon species. The simulations were performed using the Premix code of Chemkin Pro. To reduce the computational cost, mixture-averaged transport equations were utilized. Thermal diffusive effects were also included. The predictions for the laminar flame speeds of different fuel-mixtures are depicted in Figs. 35 through 38 as lines.

Results. As seen in Fig. 35, the experimental results for the neat mixtures of CO and H_2 match the model predictions very well. As expected, the syngas mixture with the greater amount of hydrogen, i.e. the bio-syngas, produced a flame speed that was on average 20.8 cm/s faster than the coal syngas mixture. Both mixtures saw a peak in flame speed around an equivalence ratio of 2.0. The experimental data for both mixtures stayed very close to the model with differences typically between about 1 and 2 cm/s.

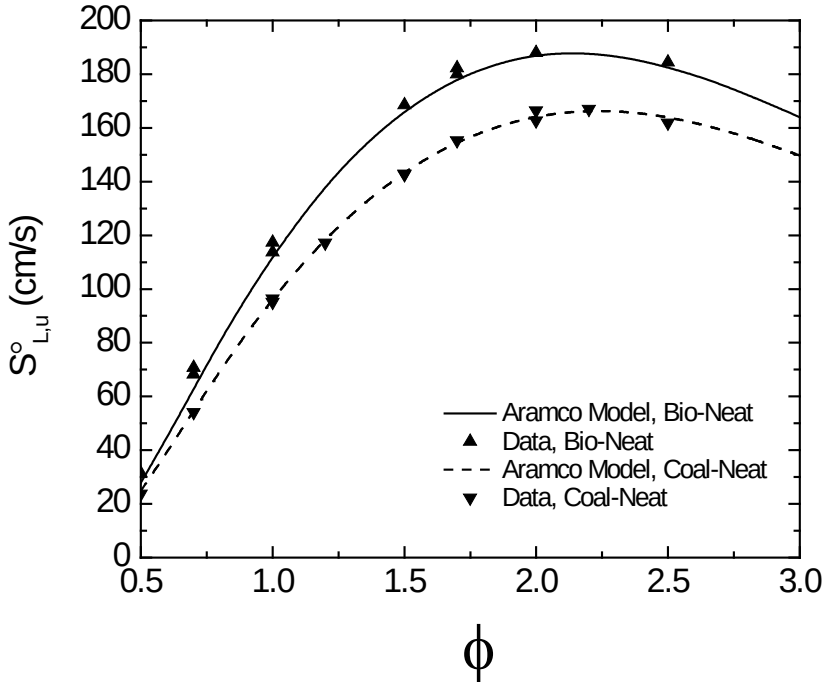

Fig. 35 Laminar flame speeds for the baseline bio-syngas and coal syngas mixtures (Bio-Neat and Coal Neat) at 1 atm and a temperature of 296 K.

As expected, the addition of hydrocarbons to the coal syngas reduced the flame speed. Figure 36 shows the model predictions and the experimental results for these syngas blends. The model predicts well the shape of the flame speed curve and predicts the peak flame speed at the correct equivalence ratio. However, the model under predicts the flame speed for all of the mixtures when hydrocarbons are added. This over prediction is most noticeable at rich mixtures when the model curves deviate from each other, and the effects of the hydrocarbons are more noticeable.

On average, the low-methane-concentration (1.6%) model under predicts the flame speed by 2.1%. The next model, with ethane (1.7%), under predicts the flame speed by 10.8%. The greatest difference was with the highest methane concentration (7.4%), which demonstrated a 17.4% average under prediction of the model. As expected, the greater percentage of hydrocarbons added to the syngas blend the greater reduction in the laminar flame speed. While the low-methane and the ethane mixtures had nearly the same concentration of hydrocarbon addition, 1.6% to 1.7% respectively, the effect of the ethane is noticeably greater.

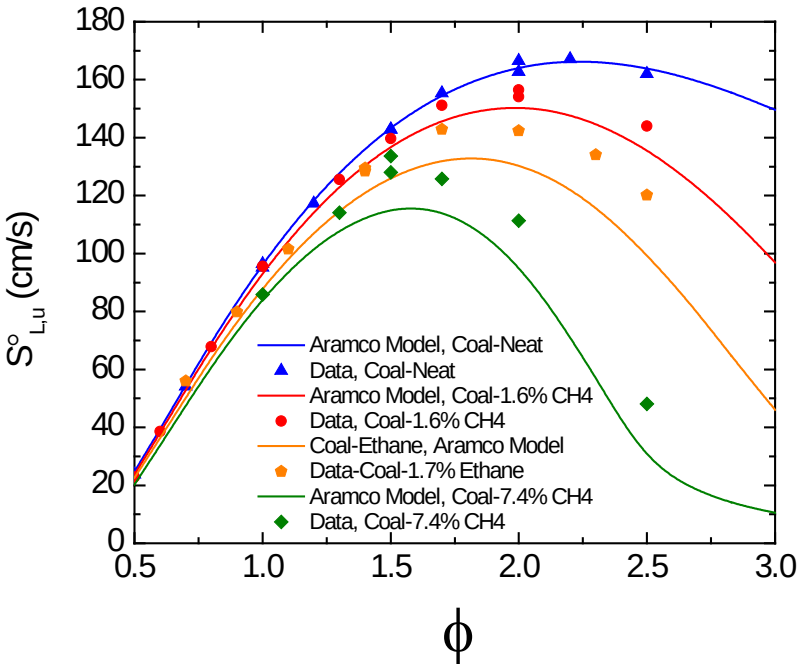

Fig. 36 Laminar flame speeds for coal syngas blends with and without hydrocarbon addition to the baseline mixture at 1 atm and a temperature of 296 K.

Like the coal syngas blends in Fig. 36, the bio-syngas blends also saw a reduction of flame speed with the addition of hydrocarbons. Also like the coal-derived blends, the peak flame speed for the bio-syngas shifted toward an equivalence ratio of 1 as more hydrocarbons were added. The experimental results are plotted in comparison to the model predictions in Fig. 37. For the bio-syngas case, ethane was added in the very small amount of 0.8%. Even in this small amount, it had a significant impact on the flame speed, with a reduction of 11.5 cm/s near the peak equivalence ratio. The model under predicted the flame speed by an average of 7.7%. The low-methane case (5%) saw a reduction in peak flame speed of 34.8 cm/s, with the peak equivalence ratio shifting from ϕ = 2.1 to 1.7. In general the model under predicts the flame speed by an average of 12.8%. This trend continues for the high-methane case (15%). Here the peak flame speed of 108.2 cm/s was found at ϕ = 1.3. The model under prediction averages 15.9% for this mixture.

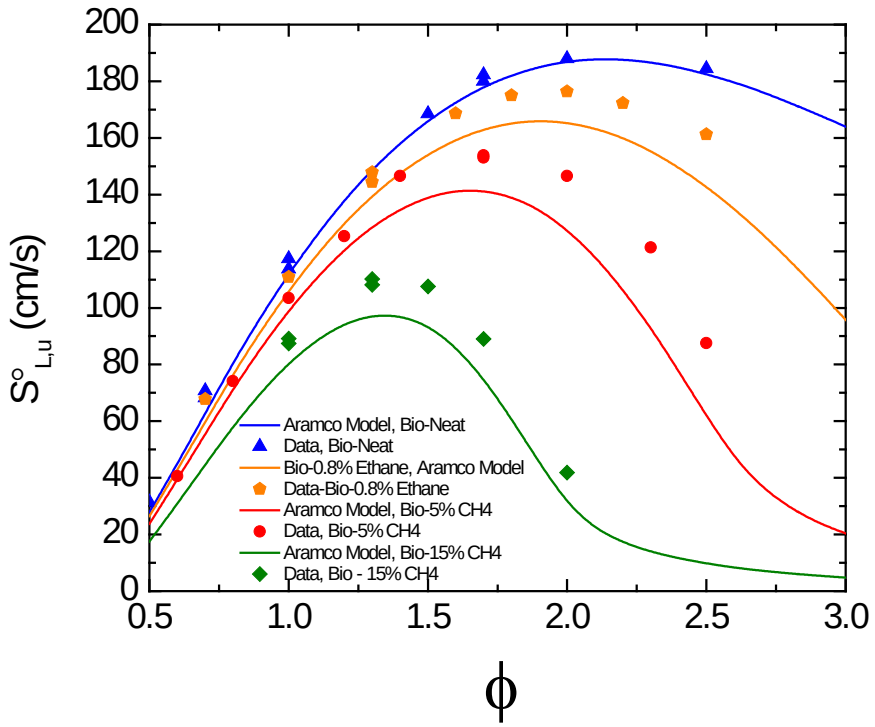

Fig. 37 Laminar flame speeds for bio-syngas blends with and without hydrocarbon addition to the baseline mixture at 1 atm and a temperature of 296 K.

Discussion. Overall, the experimental results agree well with the model predictions. This conclusion is especially true for the neat mixtures in both types of syngas fuel blends. However, the model and the data do not agree as well when methane or ethane is added. The data follow the general shape of the curve predictions, and the peak flame speeds are at the predicted equivalence ratios. On the other hand, the data significantly vary in how far away they are from the model predictions especially at rich conditions. Generally the model is very good for all lean mixtures. While this tendency has been shown for the syngas mixtures investigated in this study, it is important to show that the current model is very accurate at extreme ends of the spectrum in terms of hydrogen at the high end and methane at the lower end. Figure 38 shows the model predictions compared to previous experimental data from the authors [Krejci et al., 2013; Lowry et al., 2011] for pure hydrogen and methane flames in addition to some of the new mixtures in the present paper, the coal syngas results for comparison. As can be seen, the model does very well with pure hydrogen, the neat syngas, and pure methane. The only noticeable disagreement is in the middle when hydrocarbons are added to the syngas blend.

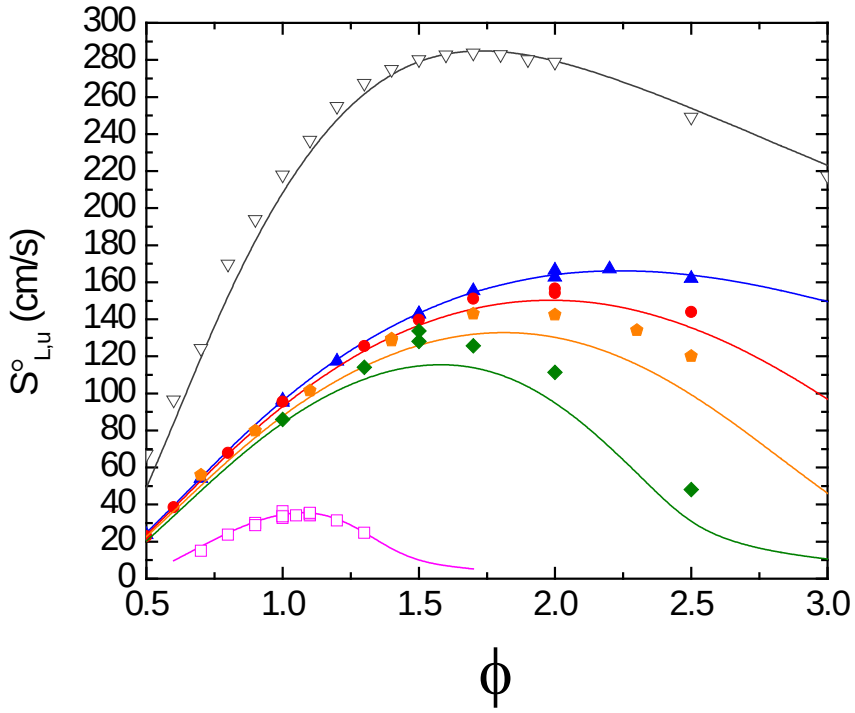

Fig. 38 Laminar Flame Speed Calculations for Hydrogen (gray) and Methane (pink) compared to the results of Coal Syngas in the current study.

Flame Speed Sensitivity Analysis. To determine the important reactions that dominate the flame speeds and control the changes in the chemistry by adding varying quantities of hydrocarbons to the syngas, mixture sensitivity analyses to flame speed were performed. CHEMKIN Pro was used to calculate the first-order sensitivity coefficients for predicting the mass flow rate. The discussions below are based on the sensitivity analyses for Coal Syngas mixtures with 0%, 1.6%, and 7.4% CH_4; and 1.7% C_2H_6, respectively. For each flame, three equivalence ratios of 0.7, 1.4, and 2.1 were selected in the sensitivity analysis to reflect the influence of increasing ϕ.

The flame speed sensitivity analyses for the pure Coal Syngas flames are shown in Fig. 39a. At $\varphi = 0.7$ and $\varphi = 1.4$, the most-sensitive reaction is $CO + OH \leftrightarrow CO_2 + H$. With CO being oxidized, OH radicals are converted to H atoms which further increase flame speed through other chain branching reactions such as $HO_2 + H \leftrightarrow OH + OH$ and $H + O_2 \leftrightarrow O + OH$. The latter reaction is of great significance in the oxidation of hydrogen and all hydrocarbons. Its sensitivity coefficient grows as the equivalence ratio increases, while most other sensitive reactions that increase the reactivity have the opposite trend. At $\varphi = 2.0$, the sensitivity coefficient to $H + O_2 \leftrightarrow O + OH$ is almost equal to that of $CO + OH \leftrightarrow CO_2 + H$. Note that in Coal Syngas the ratio of H_2:CO is 0.4:0.6, therefore higher sensitivity coefficients for this reaction are expected at corresponding conditions in the Bio Syngas flames. Its competitor for H atoms, $H + O_2 (+M) \leftrightarrow HO_2 (+M)$ has a negative sensitivity efficient at lean conditions. However, as the equivalence ratio increases this chain propagating reaction enhances reactivity because it competes with chain terminating reactions such as $H + OH + M \leftrightarrow H_2O + M$ and $HO_2 + OH \leftrightarrow H_2O + O_2$ in which the radicals recombine into molecules and decrease reactivity.

With the adoption of CH_4 in the Coal Syngas, the influence of C_1 chemistry upon the flame speed can be seen in Figs. 39b and 39c, which show the flame speed sensitivity analyses for 1.6% and 7.4% CH_4 in Coal Syngas, respectively. Although $CO + OH \leftrightarrow CO_2 + H$ remains the most-sensitive reaction under fuel-lean conditions, its importance decreases markedly as the equivalence ratio increases. In contrast, the chain branching reaction $H + O_2 \leftrightarrow O + OH$ becomes more important, especially at higher equivalence ratios when more CH_4 is adopted, as shown in Fig. 39c. This increase in importance of this reaction is mainly due to the competition from the reaction $CH_3 + H (+M) \leftrightarrow CH_4 (+M)$ induced by the addition of CH_4 to the fuel mixture. This chain terminating reaction consumes H atoms and therefore greatly decreases the reactivity, which has been shown in the experimental and simulated results as described earlier. As can be seen in Figs. 39b and 39c, this effect becomes more pronounced when the percentage of CH_4 in the fuel is higher. Meanwhile, the reaction $CH_3 + O \leftrightarrow CH_2O + H$ shows positive coefficients that increase with φ because this is the major consumption pathway for CH_3 radicals at rich conditions. Moreover, the decomposition reaction $HCO + M \leftrightarrow CO + H + M$ also contributes to the consumption of CH_3 radicals through the sequence $CH_3 + O = CH_2O + H$ and $CH_2O + R = HCO + RH$, and therefore has positive sensitive coefficients. However, the negative effect of CH_4 adoption upon flame speed dominates. The reactivity of the system gets further reduced by the oxidation of CH_4 that starts with H abstraction by the radical pool, consuming the radicals while producing CH_3 radicals.

As the equivalence ratio increases, the chain branching reaction $H + O_2 \leftrightarrow O + OH$ is further inhibited because of the lower concentration of O_2 and the enhanced competition from $CH_3 + H (+M) \leftrightarrow CH_4 (+M)$. As can be seen in Fig. 39c, at $\varphi = 2.1$, these two reactions dominate flame speed with much higher sensitivity coefficients compare to the other reactions. As a result, the flame speed is sharply decreased with increasing φ, leading to the difference between the flame speed profiles for pure Coal Syngas and that with CH_4 adopted. This trend is more obvious for the 7.4% CH_4 condition (Fig. 36), in which case the flame speed becomes very low at $\varphi > 2.5$. Note that the flame speeds for the CH_4-adopted mixtures are under-predicted by the model, while that for pure coal gas is well-predicted. This may indicate that the recombination of CH_3 radicals with H atoms, as well as other sensitive reactions such as $CH_3 + O \leftrightarrow CH_2O + H$ and H-atom abstraction reactions of CH_4 remain to be refined to improve the performance of the mechanism.

Figure 39d shows the flow rate sensitivity analysis for the 1.7% C_2H_6-adopted Coal Syngas. Although only 1.7% of C_2H_6 is added, the negative effect upon flame speed is quite obvious, as can be seen from both the analysis and the experimental observations. However, the inhibition is mainly from the C_1 chemistry, $CH_3 + H (+M) \leftrightarrow CH_4 (+M)$, while C_2 chemistry appears to be of only minor importance. This minor influence of the C_2 chemistry is because after the H abstraction of C_2H_6, the C_2H_5 radical can be readily converted into the CH_3 radical via the reaction $C_2H_5 + H \leftrightarrow CH_3 + CH_3$, which is the major consumption pathway at rich conditions. Therefore the reactions leading to the formation of C_2H_5 radicals show minor contributions to the decrease of reactivity, while the recombination of CH_3 and H plays the key role. The conversion of C_2H_5 radicals into CH_3 radicals itself also has a slight negative effect upon the reactivity because it consumes H atoms. However, CH_3 radicals are a much stronger competitor for H atoms, and two CH_3 radicals are produced from one C_2H_5 radical and an H atom. Thus, the decrease in flame speed is much more obvious than that with 1.6% CH_4 adoption. The model under-predicts the flame speed for the C_2H_6-adopted fuel, especially at high equivalence ratios.

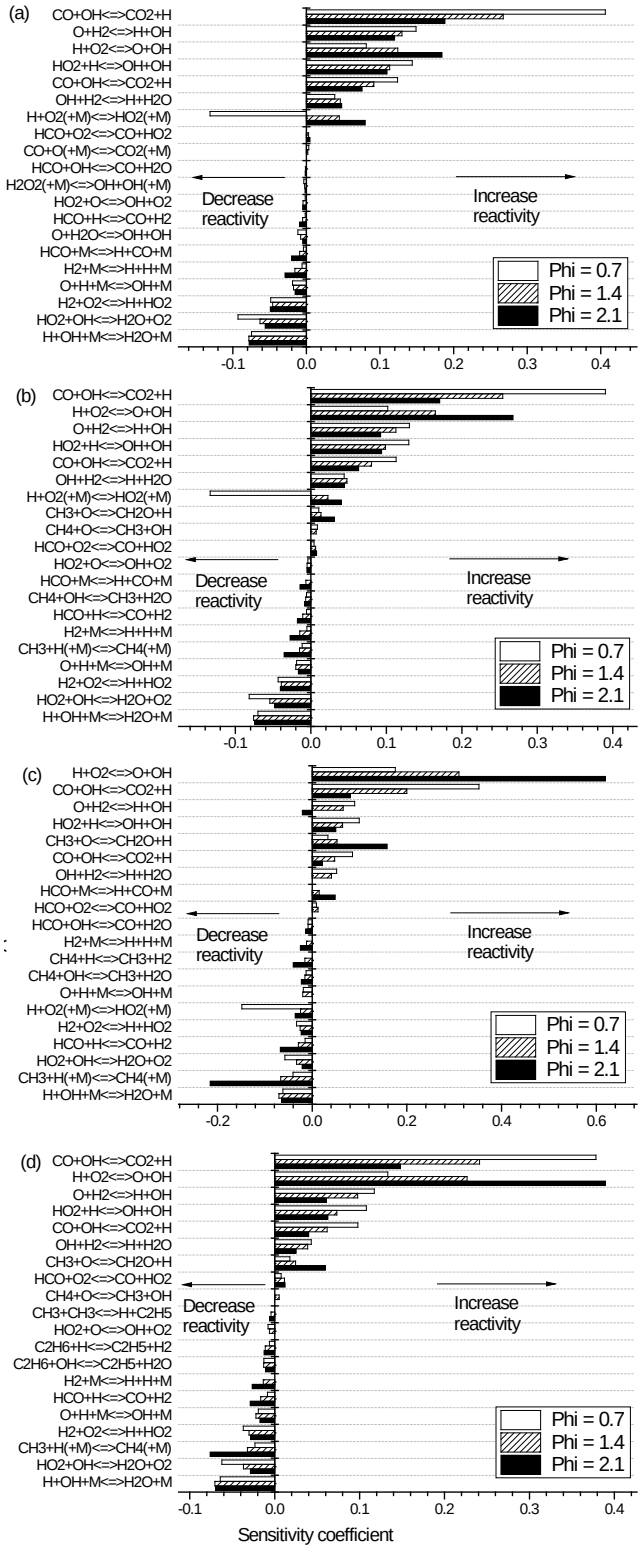

Fig. 39 Flow rate sensitivity analyses of laminar flame speeds for Coal syngas with (a) 0% CH_4, (b) 1.6% CH_4, (c) 7.4% CH_4, (d) 1.7% C_2H_6. Initial conditions 1.0 atm, 296 K, Φ = 0.7, 1.4, and 2.1.

Radiation Effects. The effects of radiation on the flame speed can also be considered. Santner et al. (2014) found the reduction in flame speed due to radiation heat loss from the flame to be small, on the order of a few percent. In the present results, the experimental data are consistently at faster flame speeds than the model predictions, indicating that if a radiation correction were included, the data would move further above (and away from) the predictions. Hence, radiation effects do not explain the current differences between data and model. For the present study, the effects of radiation are neglected.

Image Analysis. Image analysis of the growing flame showed two things. First, leaner mixtures tended to be less stable then rich mixtures, and second, hydrocarbon addition increased the stability of the flame. Figure 40 shows a small but representative selection of recorded images from a wide range of the data collected. These images are examples of trends seen throughout the data set. Note that the electrodes have been removed from the images to make the details of the flames easier to see.

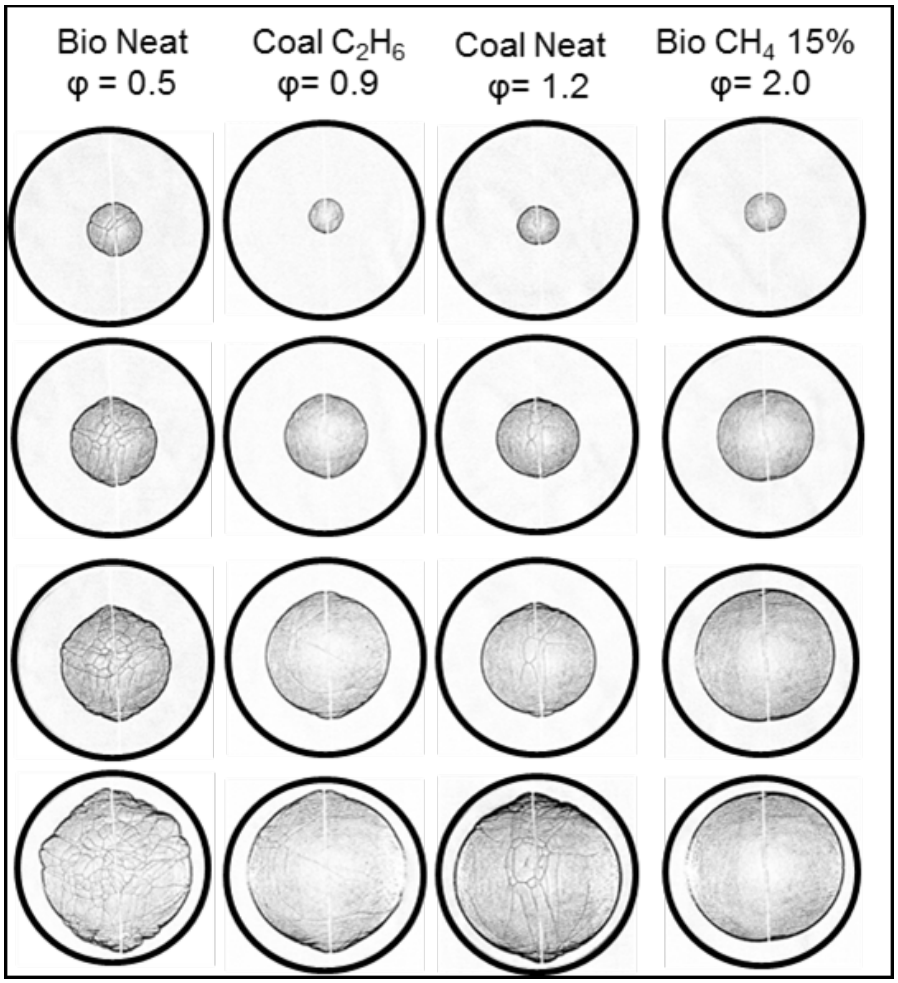

Fig. 40 Sample flame images for four different syngas blends at different equivalence ratios. Time increases in each column from top to bottom.

The flame for the neat bio-syngas blend became unstable almost immediately. This flame is the leanest condition tested, making instability expected per the Markstein lengths and Lewis numbers for these mixtures (see below). Signs of a wrinkled flame are visible in the first of the images shown. By the last images presented in Fig. 40, the flame is very wrinkled, and no longer very spherical. The two coal syngas cases presented are very similar to each other. Both are flames near ϕ = 1, with the ethane addition being a slightly lean flame ($\phi = 0.9$), and the neat case slightly rich ($\phi = 1.2$). Both of these coal syngas flames are noticeably more stable than the lean bio-syngas. The coal neat flame begins to noticeably show instabilities in the second to last image shown. The coal flame with ethane although at a leaner condition ($\phi = 0.9$) stays stable longer. There might be a slight hint of instabilities beginning in the last of the ethane coal images. The bio-syngas blend with 15% methane is the most stable. The flame stays nearly perfectly spherical throughout the images presented, with no hint of instabilities beginning. Note that the present data for un-stretched, unburned laminar flame speed were derived from the data using a method that determines numerically when the occurrence of instabilities begins to influence (i.e. accelerate) the flame propagation. Therefore, the S_L° data herein do not contain the effects of the instabilities. Further details on this data reduction procedure can be found in Lowry et al. (2011).

Markstein Length. The Markstein lengths for the coal syngas blends showed good agreement across all blends and equivalence ratios investigated. As can be seen in Fig. 41, the Markstein length averaged around 0.05 cm for all mixtures investigated. The only significant deviations from this value range were at the leanest and richest equivalence ratios investigated. Negative Markstein lengths were calculated for the neat mixture at ϕ = 0.5 and 0.7, and for the low-methane mixture at ϕ = 0.5 and 0.6. The methane added in the lower case significantly increased the Markstein length and moved the flame closer to being stable. It is also worth noting the significant increase in Markstein length for the higher methane case, at ϕ = 2.5, which was also the richest case investigated.

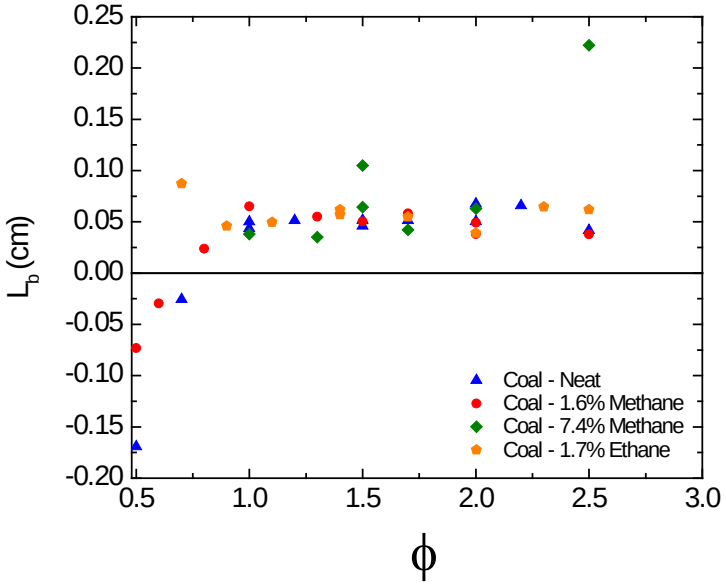

Fig. 41 Burned-gas Markstein Lengths for Coal Syngas Blends with and without hydrocarbon addition to the baseline mixture at 1 atm and initial temperature of 296 K.

The Markstein lengths for the bio-syngas mixtures investigated showed similar trends. Over a majority of the equivalence ratios investigated, all mixtures had an average Markstein length just over 0.06 cm. As can be seen in Fig. 42, the greatest variance was at the leanest and richest equivalence ratios. Like the coal syngas blend, the high-methane mixture returned a relatively large Markstein length for the richest case investigated. The Markstein lengths calculated in this study for the neat mixture are close to those reported by Prathap et al. (2008) for syngas blends.

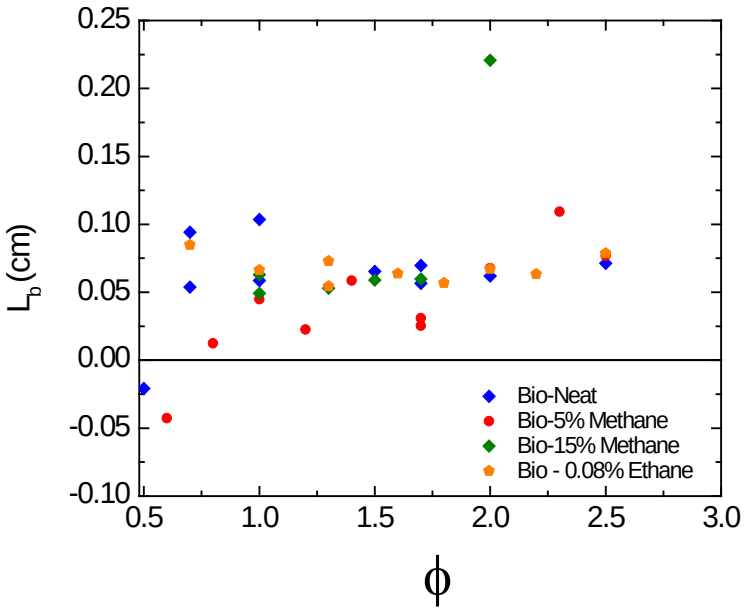

Fig. 42 Burned-gas Markstein Lengths for Bio-Syngas Blends with and without hydrocarbon addition to the baseline mixture at 1 atm and initial temperature of 296 K.

Lewis Number. Calculating the Lewis number of a fuel mixture can vary from study to study in the literature depending on the definition used. Bouvet et al. (2013) found that there were several proposed, effective Lewis number-formations that could be used in fuel mixtures. In the present study, Lewis numbers were calculated using the chemical equilibrium function in COSILAB, and the volumetric-based effective Lewis number calculation from Bouvet et al. (2013).

As was seen with the Lewis Number of pure hydrogen in air in the study by Hu et al. (2009), Le jumps from below unity to above unity as the mixture crosses $\phi = 1$. This step increase is due to the deficient species changing from the fuel in the mixture to the oxygen as the mixture stoichiometry changes from fuel lean to fuel rich.

The Lewis numbers for the coal-derived blends are shown in Fig. 43. There is very little deviation amongst the Lewis numbers of the lean mixtures. All the blends were found to have a relatively constant Lewis number throughout the lean equivalence ratios investigated, near 0.75. As hydrocarbons were added, the Lewis number slightly increased, moving it toward unity. The same trend can be seen in the bio-syngas blends, shown in Fig. 44. However as there is more hydrogen in the mixtures, and over twice as much CH_4 in the rich case, the Lewis numbers

deviate slightly more for those mixtures. The Lewis number values less than unity on the lean side tend to support the trends mentioned above wherein the leaner flames tended to be less stable.

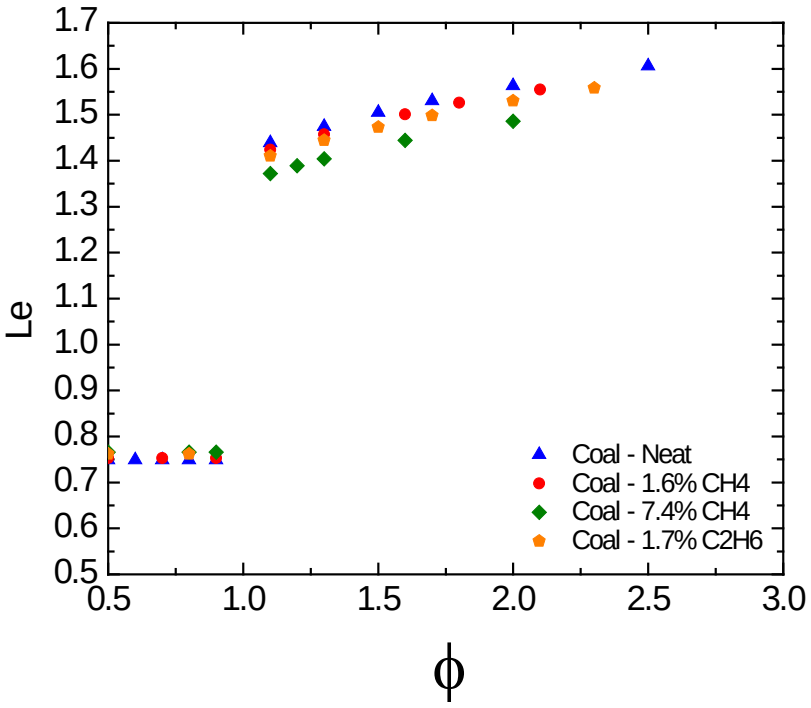

Fig. 43 Lewis Numbers for Coal Syngas Blends with and without hydrocarbon addition at various equivalence ratios at 1 atm and 296 K.

The Lewis numbers for the fuel rich equivalence ratios show a similar trend. Like the fuel lean cases, it was found that the addition of hydrocarbons moved the Lewis number closer to unity. Similar to the flame speed, the effects of the hydrocarbon addition are much clearer at the fuel rich equivalence ratios. The Lewis number was also found to increase for all mixtures as the equivalence ratio increased, ranging from values near 1.4 to 1.6 ($\phi = 2.5$).

The Lewis Number of all syngas mixtures in this study is closer to 1.0 than are the Lewis numbers for pure Hydrogen reported in Hu et al. (2009). For their lean mixtures, they found the Lewis number to be around 0.3, and for the rich mixtures around 2.0. Therefore, the most-significant impact on the Lewis number is the addition of the carbon monoxide, which also has a significantly greater concentration in the fuel blends then any of the hydrocarbons added to the neat syngas mixtures.

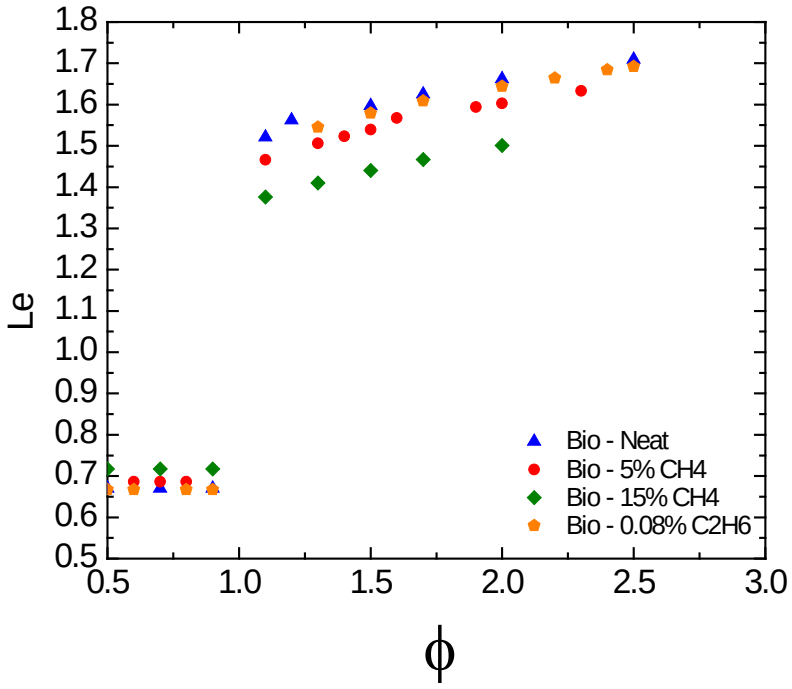

Fig. 44 Lewis Numbers for Bio-Syngas Blends with and without hydrocarbon addition at various equivalence ratios at 1 atm and 296K.

TASK 4 – DESIGN AND CONSTRUCTION OF A HIGH-PRESSURE TURBULENT FLAME SPEED FACILITY

Progress in this task included background calculations, planning, and the start of the detailed design of the new apparatus. A review of the conceptual design is provided as follows.

Background

The flame speed bombs can be classified as open or closed volume systems regarding the mass movement across the vessel enclosure during the flame growth. In a closed-volume bomb, as the name implies, the mass is trapped in the bomb and remains constant from the moment the fuel and oxidizer input ports are closed until the combustion products are evacuated. A closed-volume bomb must be designed to withstand the pressure developed by thermal energy released by combustion, which is typically 7 to 10 times higher than the initial pressure. In an open system, during the flame growth process, the gases are allowed to escape from the bomb to avoid the pressure build. In principle, if the gases are vented as fast as they are expanding, the pressure peak can be limited.

It is challenging to design a flame bomb because it must safely contain a sudden pressure surge, but also provide access ports to perform measurements, including windows for imaging, laser diagnostics and optical techniques. The complexity is augmented as higher initial pressures are attempted at intense turbulence levels, in an effort to reproduce conditions relevant to practical devices such as gas turbine combustors. Nonetheless, the objective of this work is to design a fan-stirred vented bomb to perform turbulent flame speed measurements at initial pressures above atmosphere.

Expansion tank

The vented gases from the bomb will be discharged into a second chamber or expansion tank. The expansion tank should be able to receive the burst of gases ejected from the bomb while keeping the pressure sufficiently low. Mass and energy conservation assumptions in a closed system are invoked to propose a tank size. The system, in this case, comprises both the expansion tank and the flame bomb. No dynamic considerations are accounted in the expansion tank sizing, only equilibrium. It is also assumed that all the fuel in the combustible mixture is completely consumed. For the purpose of this design, the worst-case scenario is considered to be a rich mixture hydrogen and air with an equivalence ratio of 4.0 at 30 atm pressure prior to ignition.

Figure 45 show the equilibrium pressure of the expansion tank as function of the relative size. Two initial expansion tank pressures are plotted, namely 1 and 30 atm. An expansion tank 30 times larger than the flame bomb held at initial pressure of one atmosphere prior to ignition was deemed an adequate solution for vented experiments. This expansion tank selection also affects the type of pressure release device needed to vent the contents of the bomb since a significant pressure gradient is implied for experimental pressure above one atmosphere.

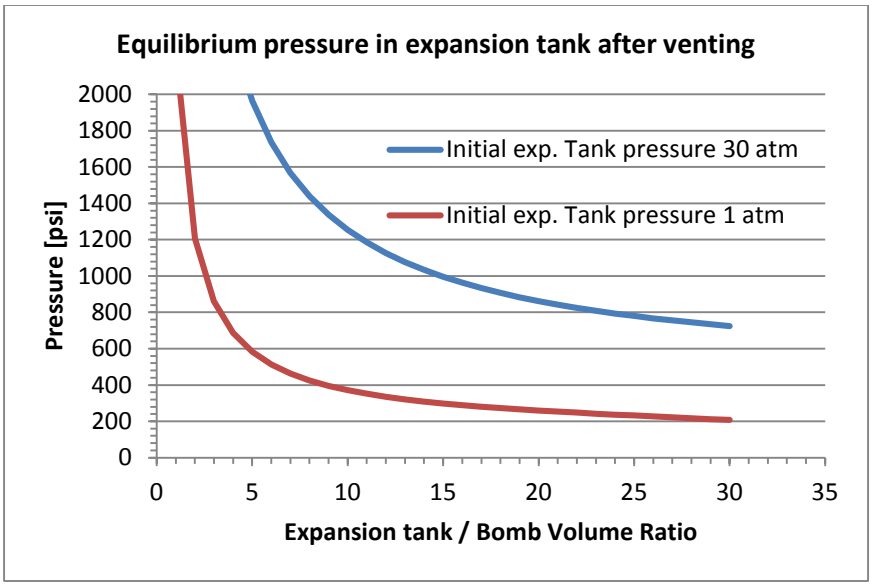

Fig. 45 Final pressure of expansion tank after receiving vented gases at two different initial pressures.

Vent sizing

Proper vent sizing is of the essence in vented deflagrations. If the vent is too small, the gases will not escape at a fast enough rate to prevent pressure accumulation in the bomb. There is not a unique or a universally accepted methodology in the combustion and safety community to size a vent. Razus et al. (2001) compared several calculation methods with experimental data for vents that discharge directly to the atmosphere, while Russo and Di Benedetto (2007) did something similar for vents that are discharged through ducts. More recently, Lautkaski (2011) reviewed the literature available for venting deflagrations, including the correlation for high initial pressures developed by Molkov (2001).

Molkov proposed a correlation to predict the maximum overpressure in vented deflagrations with initial pressure above one atmosphere [Molkov, 2001]. Molkov's correlation was calibrated with a set propane of experimental data at quiescent and turbulent conditions with initial pressures ranging from 1 to 7 atmospheres obtained by Pegg et al. (1992). The model relates two dimensionless numbers, namely a reduced pressure and the Bradley number. The dimensionless reduced pressure P_M, is defined as the ratios of initial, venting and maximum pressure attained in the vented deflagration. The Bradley number depends on key parameters such as the of the mixture sound and flame speed at initial conditions, the volume of the bomb, the area of the vent and the influence of the outflow in the surface area of the flame.

Figure 46 redraws a graphic originally published by Molkov (2001) with experimental results of Pegg et al. (1992) and Chaineaux, J., and E. Dannin (1992). The model was calibrated with the data shown in open symbols. The results from Chaineaux, J., and E. Dannin, closed symbols, are fairly predicted but exhibit more scatter when compared with the model. Figure 47 shows a view of the current design concept.

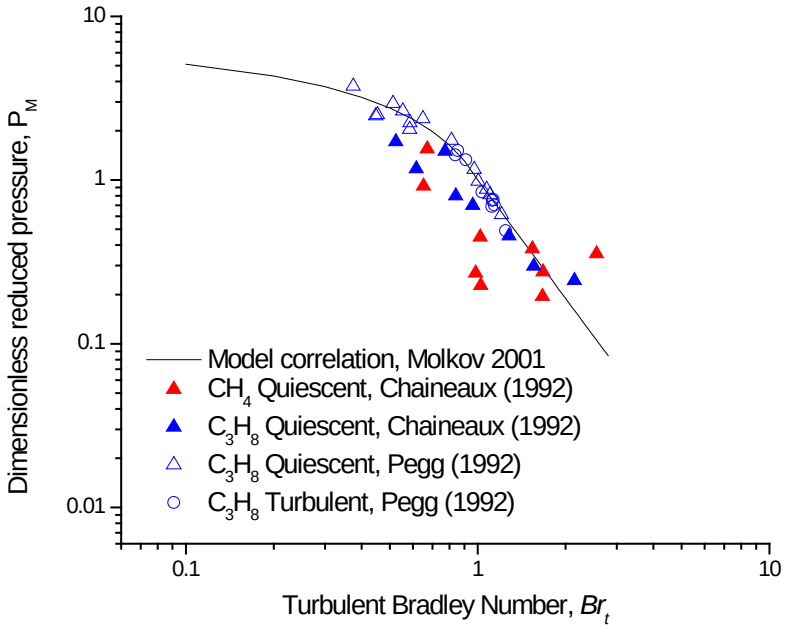

Fig. 46 The experimental values of dimensionless reduced pressure, P_M, and turbulent Bradley Number, Br_t (Molkov 2001) redrawn. The test data by Pegg et al. (1992) is shown with open symbols and those by Chaineaux and Dannin (1992) with closed symbols.

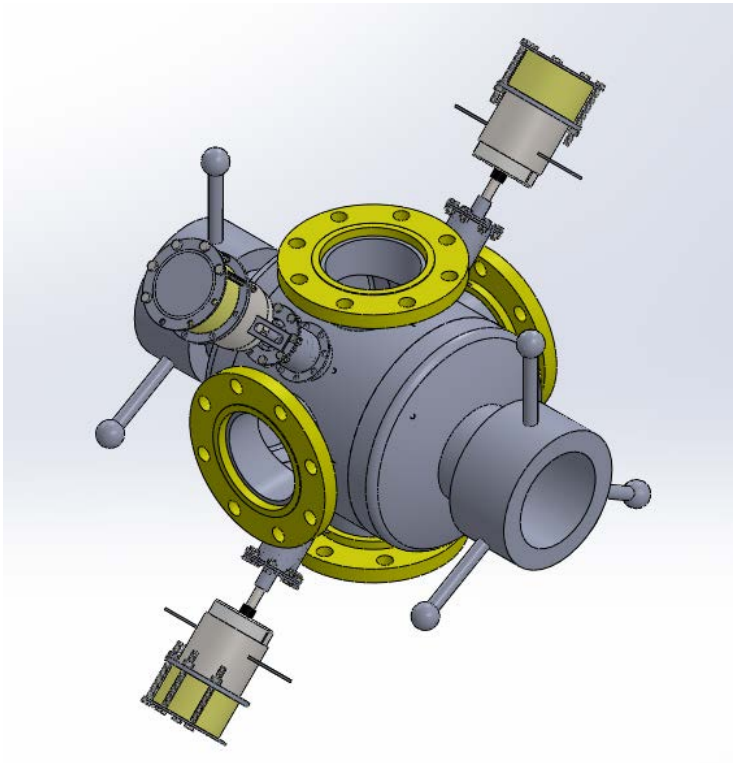

Fig. 47 Fan-stirred vented flame bomb, conceptual sketch. Double vent with breech loaders and 4 windows.

TASK 5 – HIGH-PRESSURE TURBULENT FLAME SPEED MEASUREMENTS

This task is slated to begin in the ninth quarter (Year 3).

CONCLUSIONS

The effects of impurities on fundamental combustion properties of premixed systems fueled with bio- or coal-derived syngases were investigated over a wide range of conditions relevant to gas turbine combustion. The results of this study show that not all the impurities have an effect on the ignition delay time or laminar flame speed. The concentration of the impurities, the temperature, and the pressure are also important factors governing the influence of impurities. While the effects of impurities are typically less important than for hydrocarbons, these effects appear to be linked to the chemistry only, as no noticeable flame temperature change was observed. NO_2 showed some promoting effects on the ignition delay time at conditions where the HO_2 radical was dominating. For the high-temperature flame speed process, HO_2 radicals do not play an important role, explaining the lack of effect of NO_2 on the laminar S_L. When H_2S, NH_3, and HCN are in the mixture, they will tend to react with H radicals and to produce radicals that present a lower reactivity than OH, hence reducing the reactivity of the mixture by limiting r1 ($H + O_2 \rightleftarrows OH + O$). However, H_2S will also have a promoting effect on the ignition delay time for conditions where the HO_2 radical is important (low-temperature, high-pressure conditions for the ignition delay time predictions). This lower-temperature behavior is due to a decrease in the r2 pathway ($H + O_2 + M \rightleftarrows HO_2 + M$) due to the reaction r6 ($H_2S + H \rightleftarrows SH + H_2$) followed by enhancing reactions (compared to r2) that will lead to r10 ($O + H_2 \rightleftarrows OH + H$).

COS and SO_2 are the only impurities that do not exhibit any effect on both the syngas laminar flame speed and the ignition delay time under the conditions investigated. One can conclude that these two species can be neglected for realistic syngas mixtures at gas turbine conditions.

Hydrocarbon addition significantly impacts the flame speed of syngas blends. This decelerating effect is especially noticeable for rich mixtures. The model does a very good job of predicting the flame speed for the syngas mixtures in the neat case. When hydrocarbons are added, the model still does a good job of predicting the general shape of the curve and accurately predicts the equivalence ratio of the peak flame speed. However, experiments found that when hydrocarbons were added, the model under predicts the flame speed by several percent. This under prediction is especially noticeable at the richer mixtures. While the current Aramco model under predicts the flame speed for syngas with hydrocarbon addition, it still does a very good job for the pure fuels involved.

Analysis of the flame images found that lean mixtures were typically less stable than the fuel rich ones. The addition of hydrocarbons was found to noticeably increase the flame stability. Hydrocarbon addition however was found to have little impact on the burned-gas Markstein lengths of the mixtures. The leanest mixtures tested were the only ones to show a negative Markstein length. On average, all mixtures had a consistent Markstein length with the bio-syngas mixtures having a noticeably wider deviation. The Lewis numbers of the mixtures were found to also be consistent. For the leaner cases, there was almost no change as hydrocarbons were added, although there was a slight change toward unity Lewis Number. For the rich mixtures, the Lewis number moved noticeably closer to 1.0 as hydrocarbons were added. In general, hydrocarbon addition seems to increase the stability of the flame. This result of hydrocarbon addition to the syngas mixture is especially important in the fuel lean regions which will typically be used in gas turbine and other industrial applications.

Detailed design of the new turbulent flame speed vessel continues, and a summary of the progress over the first year and the current status was provided in this report. The basic design of the high-pressure turbulent flame speed vessel will be a vented system, and the sizing of the exhaust volume and port area was completed.

Three journal papers and six conference papers related to the present effort were completed during this first project year. In addition, the PI presented one of the papers, and students presented several posters at the 35th International Symposium on Combustion in San Francisco in August, 2014.

REFERENCES

Bouvet, N., Halter, F., Chauveau, C., Yoon, Y. (2013) "On the effective Lewis number formulations for lean hydrogen/hydrocarbon/air mixtures" International Journal of Hydrogen Energy **38** pp. 5949-5960.

Burke, M. P., Qin, X., Ju, Y., and Dryer, F. L. (2007) "Measurements of Hydrogen Syngas Flame Speeds at Elevated Pressures," 5th U.S. Combustion Meeting.

Cayana, F.M., Zhi, M., Pakalapati, S.R., Celik, I., Wu, N., and Gemmen, R. (2008) "Effects of coal syngas impurities on anodes of solid oxide fuel cells". J. Power Sources 185, 595-602.

Chaineaux, J. and E. Dannin (1992) "Sizing of explosion vents for the protection of vessels in which gases are processed at pressure and temperature higher than ambient," *Proceedings of loss prevention and safety promotion in the process industries*, Taormina, pp. 1-30.

Chen, Z. (2010) "On the extraction of laminar flame speed and Markstein length from outwardly propagating spherical flames" Combust. Flame **158** (2) pp. 291-300.

Cuoci, A., Frassoldati, A., Buzzi Ferraris, G., Faravelli, T., and Ranzi, E. (2007) "The ignition, combustion and flame structure of carbon monoxide/hydrogen mixtures. Note 2: Fluid dynamics and kinetic aspects of syngas combustion". Int. J. Hydrogen Energy 32, 3486-3500.

Dagaut, P., Glarborg, P., and Alzueta M. U. (2008) "The oxidation of hydrogen cyanide and related chemistry". Prog. Energy Combust. Sci. 3, 1-46.

Das, A. K., Kumar, K., and Sung, C.-J. (2011) "Laminar Flame Speeds of Moist Syngas Mixtures," Combust. Flame, 158, pp. 345-353.

Glarborg, P. (2007) "Hidden interactions - Trace species governing combustion and emissions". Proc. Combust. Inst. 31, 77–98.

Glarborg, P. and Marshall, P. (2013) "Oxidation of Reduced Sulfur Species: Carbonyl Sulfide". International Journal of Chemical Kinetics 45, 429–439.

Herzler, J., Herbst, J., Kick, T., Naumann, C., Braun-Unkhoff, M., and Riedel, U. (2012) "Alternative Fuels Based on Biomass: an Investigation of Combustion Properties of Product Gases". Proceedings of ASME Turbo Expo 2012, GT2012, paper GT2012-69282.

Hu, E., Huang, Z., He, J., and Miao, H. (2009) “Experimental and numerical study on laminar burning velocities and flame instabilities of hydrogen-air mixtures at elevated pressures and temperatures” International Journal of Hydrogen Energy **34** pp. 8741-8755.

Kéromnès, A., Metcalfe, W. K., Donohoe, N., Das, A. K., Sung, C. J., Herzler, J., Naumann, C., Griebel, P., Mathieu, O., Krejci, M. C., Petersen, E., Pitz, W. J., and Curran, H. J. (2013) “An Experimental and Detailed Chemical Kinetic Modelling Study of Hydrogen and Syngas Mixtures at Elevated Pressures,” Combustion and Flame 160, 995-1011.

Krejci, M.C., Mathieu, O., Vissotski, A.J., Ravi, S., Sikes, T.G., Petersen, E.L., Kéromnès, A., Metcalfe, W., and Curran, H.J. (2013) “Laminar Flame Speed and Ignition Delay Time Data for the Kinetic Modeling of Hydrogen and Syngas Fuel Blends”. J. Engineering for Gas Turbines and Power, 135 / 021503-1.

Lautkaski, R. and T. Vanttola (2011) *Duct Venting of Gas Explosions,* VTT Technical Research Centre of Finland.

Lee, H.C., Jiang, L.Y., and Mohamad, A.A. (2014) “A review on the laminar flame speed and ignition delay time of Syngas mixtures” International Journal of Hydrogen Energy **39** pp. 1105-1121.

Lowry, W., de Vries, J., Krejci, M., Petersen, E., Serinyel, Z., Metcalfe, W., Curran, H., Bourque, G. (2011) “Laminar Flame Speed Measurements and Modeling of Pure Alkanes and Alkane Blends at Elevated Pressures” Journal of Engineering for Gas Turbines and Power **133** pp. 091501-1 – 091501-9.

Mathieu, O., Levacque, A., and Petersen, E. L. (2012) “Effects of N_2O addition on the ignition of H2–O2 mixtures: Experimental and detailed kinetic modeling study”. International Journal of Hydrogen Energy 37, 15393-15405.

Mathieu, O., Kopp, M. M., and Petersen, E. L. (2013a) “Shock Tube Study of the Ignition of Multi-Component Syngas Mixture With and Without Ammonia Impurities,” Proc. Combust. Inst. 34, pp. 3211-3218.

Mathieu, O., Petersen, E. L., Heufer, A., Donohoe, N., Metcalfe, W. K., Curran, H. J., Güthe, F., Bourque, G. (2013b) “Numerical Study on the Effect 1 of Real Syngas Compositions on Ignition Delay Times and Laminar Flame Speeds at Gas Turbine Conditions”. J. Eng. Gas Turbines Power, DOI: 10.1115/1.4025248.

Mathieu, O., Levacque, A., and Petersen, E. L. (2013c) "Effects of NO_2 addition on hydrogen ignition behind reflected shock waves". Proceedings of the Combustion Institute 34, 633-640.

Mathieu, O., Deguillaume, F., and Petersen, E. L. (2013d) Effects of H_2S addition on hydrogen ignition behind reflected shock waves: Experiments and modeling. Combustion and Flame, http://dx.doi.org/10.1016/j.combustflame.2013.07.011.

Mathieu, O., Hargis, J.W., Petersen, E.L., Bugler, J., Curran, H.J., and Güthe, F. (2014a), "The Effect of Impurities on Ignition Delay Times and Laminar Flame Speeds of Syngas Mixtures at Gas Turbine Conditions" ASME Paper GT2014-25412, Proceedings of ASME Turbo Expo 2014, June 16-20 2014, Düsseldorf, Germany.

Mathieu, O., Petersen, E.L., Heufer, A., Donohoe, N., Metcalfe, W., Curran, H.J., Güthe, F., and Bourque, G. (2014b) "Numerical Study on the Effect of Real Syngas Compositions on Ignition Delay Times and Laminar Flame Speeds at Gas Turbine Conditions," Journal of Engineering for Gas Turbines and Power **136** pp. 011502-1-011502-9.

Metcalfe, W. K., Burke, S. M, Ahmed, S. S, and Curran, H. J. (2013) "A Hierarchical and Comparative Kinetic Modeling Study of C1–C2 Hydrocarbon and Oxygenated Fuels. Int. J. of Chem. Kinetics 45, pp. 638-675.

Molkov, V.V. (2001) "Unified correlations for vent sizing of enclosures at atmospheric and elevated pressures," *Journal of Loss Prevention in the Process Industries*, 14(6): pp. 567–574.

Munasinghe, P. C. and Khanal, S. K. (2010) "Biomass-Derived Syngas Fermentation into Biofuels: Opportunities and Challenges," Bioresour. Technol., 101, 5013–5022.

Natarajan, J., Nandula, S., Lieuwen, T., and Seitzman, J. (2005) "Laminar Flame Speeds of Synthetic Gas Fuel Mixtures," ASME Paper GT2005-68917.

Newby, A., Smeltzer, E. E., Lippert, T. E., Slimane, R. B., Akpolat, O. M., Pandya, K., Lau, F. S., Abbasian, J., Williams, B. E., and Leppin, D. (2001) "Novel Gas Cleaning/Conditioning for Integrated Gasification Combined Cycle Base Program," Report No. DE-AC26-99FT40674.

Pegg, M., P. Amyotte, and S. Chippett (1992) "Confined and vented deflagrations of propane/air mixtures at initially elevated pressures," in *Proc. 7-th Intern. Symp. Loss Prevention in the Process Industries,* Taormina, Italy.

Prathap, C., Ray A., and Ravi, M. R. (2008) “Investigation of Nitrogen Dilution Effects on the Laminar Burning Velocities and Flame Stability of Syngas Fuel at Atmospheric Condition,” Combust. Flame, 155, pp. 145-160.

Ravi, S., Peltier, S. J., and Petersen, E. L. (2013) “Analysis of the Impact of Impeller Geometry on the Turbulent Statistics inside a Fan-Stirred, Cylindrical Flame Speed Vessel using PIV,” *Experiments in Fluids*, Vol. 54, pp. 1424.

Razus, D.M. and U. Krause (2001) “Comparison of empirical and semi-empirical calculation methods for venting of gas explosions,” *Fire Safety Journal*, **36**(1): pp. 1-23.

Russo, P. and A. Di Benedetto (2007) “Effects of a Duct on the Venting of Explosions - Critical Review,” *Process Safety and Environmental Protection*, **85**(1): p. 9-22.

Santner, J., Haas, F. M., Ju, Y., Dryer, F. L. (2014) “Uncertainties in interpretation of high pressure spherical flame propagation rates due to thermal radiation” Combustion and Flame **161** pp. 147-153.

Sharma, S. D., McLennan, K., Dolan, M., Nguyen, T., and Chase, D. (2013) “Design and Performance Evaluation of Dry Cleaning Process for Syngas,” Fuel, 108, 42–53.

Sivaramakrishnan, R., Brezinsky, K., Dayma, G., and Dagaut, P. (2007) “High pressure effects on the mutual sensitization of the oxidation of NO and CH_4–C_2H_6 blends” Phys. Chem. Chem. Phys. 9 4230–4244.

Trembly, J. P., Gemmen, R. S., and Bayless, D. J. (2007) “The effect of IGFC warm gas cleanup system conditions on the gas–solid partitioning and form of trace species in coal syngas and their interactions with SOFC anodes”. Journal of Power Sources 163, 986–996.

Wang, J., Zhang, M., Huang Z., Kudo, T., and Kobayashi, H. (2013) “Measurement of the instantaneous flame front structure of syngas turbulent premixed flames at high pressure”. Combust. Flame 160, 2434-2441.

Xu, Z.-R., Luo, J.-L., and Chuang, K. T. (2009) “The Study of Au/MoS2 Anode Catalyst for Solid Oxide Fuel Cell (SOFC) Using H2S-Containing Syngas Fuel,” J. Power Sources, 188, 458–462.

Xu, D., Tree, D.R., Randy S., and Lewis, R.S. (2011) “The effects of syngas impurities on syngas fermentation to liquid fuels”. Biomass and Bioenergy 35, 2690-2696.